UNCLASSIFIED

AD 404 028

UNCLASSIFIED

STANFORD RESEARCH INSTITUTE | (*SRI)

MENLO PARK CALIFORNIA

April 30, 1963

Technical Report

RADIATIVE ENERGY TRANSFER FROM NUCLEAR DETONATIONS ABOVE

50-KM ALTITUDE

Prepared for:

OFFICE OF CIVIL DEFENSE
DEPARTMENT OF DEFENSE
WASHINGTON 25, D.C.

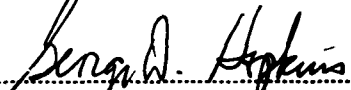CONTRACT NO. OCD-OS-62-135

By: R. I. Miller   T. O. Passell

SRI Project No. IMU-4021-302

Approved:

R. B. VAILE, JR., DIRECTOR
PHYSICS DIVISION

GEORGE D. HOPKINS, MANAGER
OPERATIONS ANALYSIS

Copy No. 143

CONTENTS

FIGURES

FIGURES

SUMMARY OF RESULTS

This theoretical study examines the expected thermal radiation from nuclear weapons detonated at very high altitudes within the atmosphere (50-80 km) or in outer space (greater than 80-km altitude). From the standpoint of ground effects, the very high altitude airburst is initially an intense flash of x-rays. These invisible rays have little power of penetration and are encapsulated by a sphere of air molecules immediately surrounding the detonation point. As the fireball expands and transfers its energy to a larger and larger mass of air, it finally cools to a temperature $(20,000^{\circ}K)$ at which the radiation can penetrate the surrounding air. At this point the fireball ceases to expand and begins to radiate ultraviolet, visible, and energy of longer wavelengths.

An ozone layer at 20-40 km altitude protects the earth from the destructive effects of ultraviolet rays from the sun. In the same way, much of the fireball emission is absorbed by the ozone layer especially as the fireball cools from $20,000^{\circ}K$ to $10,000^{\circ}K$. The ozone layer is never heated to incandescence, however, so the absorption by the ozone layer goes unnoticed on the ground.

In spite of the ozone layer, much of the fireball thermal emission begins reaching the ground as the fireball temperature drops below about $20,000^{\circ}K$. By the time the fireball has reached $5000^{\circ}K$ other cooling processes compete with radiation and most thermal radiation ceases at this point.

To determine ground effects one must know where the fireball is. For burst heights from 50 to 80 km the problem is simple; the fireball is approximately a sphere surrounding the burst point. Above 80 km it is not so simple to know the shape and position of the fireball. Figure S-1 illustrates the fireball (region of primary incandescence) for five different burst heights, 49 km, 63 km, 98 km, and 119 km. The solid dots represent the detonation points. The solid line enclosing the cross hatched area represents the region where the x-ray flash initially deposited its energy by absorption in the air. The dotted enclosures represent the subsequent slight growth of the initial fireball which occurs if the x-ray flash produced initial temperatures above $20,000^{\circ}K$.

The initial temperature of the device determines to what altitude level the x-rays will penetrate to release their energy. We considered three possible levels within the feasible range for devices at initial temperatures around 10^7 °K.[1]* These three levels were 70 km, 83 km, and 95 km -- corresponding to arbitrarily chosen air densities of 10^{-7}, 10^{-8}, and 10^{-9} grams/cm^3, respectively. There is a device temperature which is optimum for heating each of the above layers. But <u>heating is</u> not the only consideration. The heat must be able to radiate fast enough to compete with other cooling processes such as convection.

We now consider which one of the three layers is most worthy of detailed computation by reason of its ability to radiate once heated. On this basis alone the choice would have to be the 10^{-7} g/cm^3 layer (70 km) since it is the most dense. We note, however, that the 70-km layer requires ten times more yield (the yields are all in the megaton range) to heat it to the threshold of incandescence that is required for the 10^{-8} g/cm^3 layer. The 10^{-9} g/cm^3 layer is definitely eliminated because its opacity to its own radiant emission is too low to allow radiation to compete with convection. Therefore, the 10^{-8} g/cm^3 layer was chosen for detailed computation since it can be efficiently heated to incandescence while being dense enough to reradiate its energy before convection predominates (several seconds). The device temperature optimum for heating this level is 1.45×10^7 °K.

The device temperature assumed above essentially determines the fireball ceiling at 80 km shown in Fig. S-1. No fireball can exist above this altitude region. A curious corollary is that as detonation altitudes increase above 80 km the fireball and detonation point part company.

The spatial extent of the fire-pancakes of Fig. S-1 can be described roughly as shallow cones with base radii of roughly (h-80) km and vertical thicknesses of around 10-15 km (h is the burst height in kilometers).

---

* Superscripts refer to references collected at the end of this report.
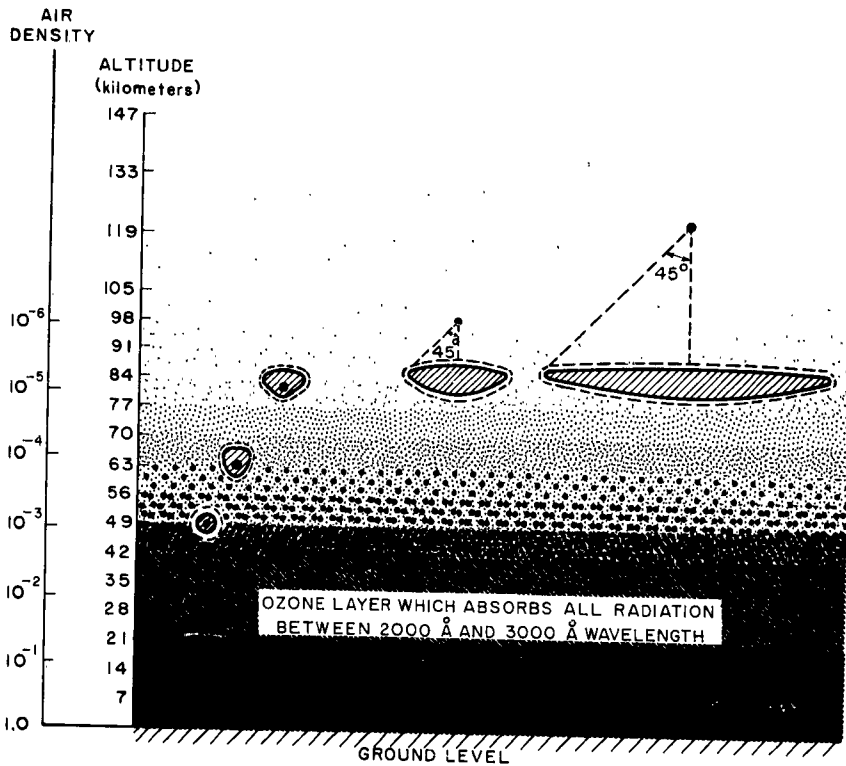
FIG. S-1 THE APPROXIMATE SHAPE AND LOCATION OF THE FIREBALL FOR VERY HIGH-YIELD NUCLEAR DETONATIONS AT FIVE ARBITRARILY SELECTED ALTITUDES FROM 49 km TO 119 km

The numerical results for ground effects are summarized in Figs. S-2 and S-3. They contain all the information needed to compute the energy flux received at any point on the ground from a nuclear detonation above 50-km altitude. The energy flux calculated is that which would be received on a surface oriented to receive the maximum possible radiation, i.e., facing the fireball. Figure S-2 gives the yield required at a given burst height for energy fluxes at ground zero of 100, 10, and 5 cal/cm², assuming 100% transmission by the atmosphere within its assumed transparent window (3100A-19,000A). Since the time behavior of the energy arrival is often of interest, separate curves are given for the energy arriving in the first 1-sec period and in the first 10-sec period, respectively, after detonation.

Figure S-3 gives the fractional energy flux received at all points on the ground relative to that received at ground zero. The distance of the particular point of interest from ground zero is given in units of burst heights. For example, if the burst height were 100 km, the number 1 on the abscissa of Fig. S-3 would correspond to a point 100-km from ground zero.

To illustrate the use of Figs. S-2 and S-3, consider a specific example. Suppose we wish to know how far from ground zero would an optimally oriented surface receive 10 cal/cm² in the 1-sec period after detonation of a 150-mt device at 200-km altitude. Entering Fig. S-2 along the horizontal line Y = 150 mt, we proceed to h = 200 km. We observe that the contour for receiving 5 cal/cm² in the first 10-sec period after detonation passes just above the 200-km, 150-mt intersection. Thus we conclude such a device cannot deliver 10 cal/cm² <u>anywhere</u> on the ground within 10 sec (let alone 1 sec) since Fig. S-3 clearly shows that ground zero always receives more energy than any other ground point.

Consider a second example. Suppose a device of 100-mt yield is detonated at 80-km altitude. To what distance from ground zero do optimally oriented surfaces receive 10 cal/cm² in the 1-sec following detonation? Entering Fig. S-2 on the vertical line at 80-km burst height, we observe that the 1-sec and the 10-sec curves have merged and that 320 mt gives 100 cal/cm² at ground zero. Since the S_0 curves are linear
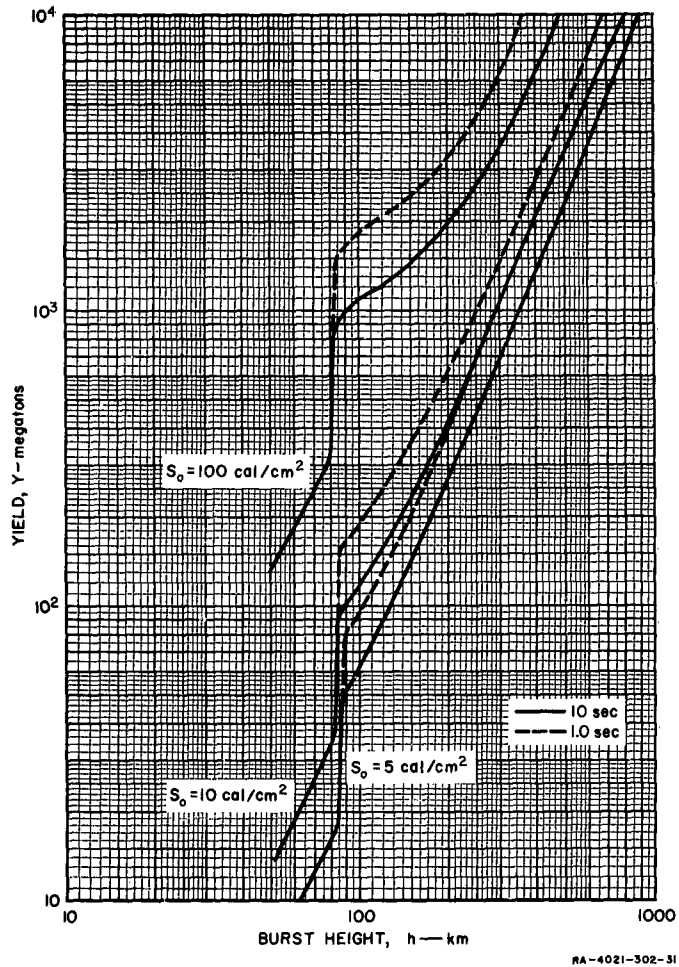
FIG. S-2 THE YIELD REQUIRED AT A GIVEN BURST HEIGHT FOR THREE
ENERGY FLUXES DELIVERED TO A HORIZONTAL SURFACE AT
GROUND ZERO WITHIN 1 AND 10 sec AFTER DETONATION
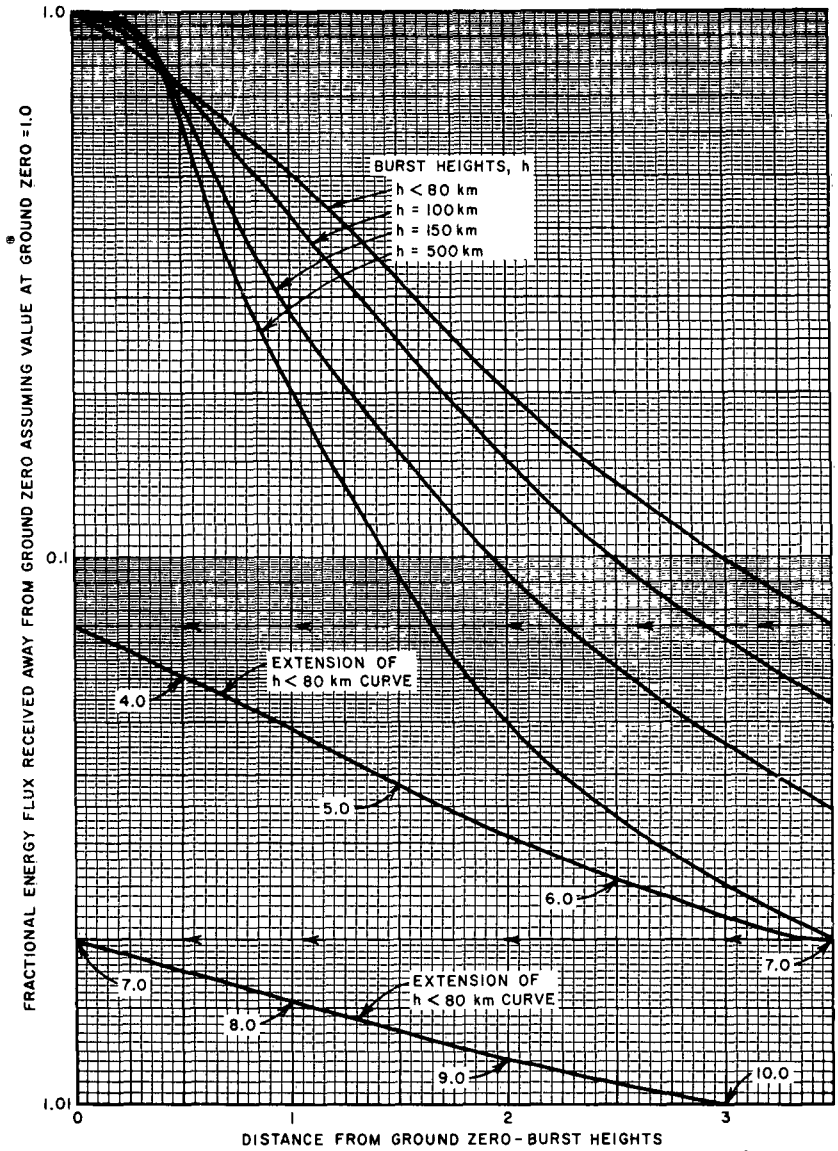
FIG. S-3   ENERGY FLUX RECEIVED IN OPTIMALLY ORIENTED SURFACES
AS A FUNCTION OF DISTANCE FROM GROUND ZERO

RB-4021-302-46

with yield below 100 km, S_o for 100 mt becomes 100/320 x 100 or 31.3 cal/cm^2. Now that we have the value for ground zero, we wish to know how far from ground zero one must proceed to reduce the energy flux to 10 cal/cm^2. The relative reduction is to 0.32 or 32% of the value at ground zero. Using the h < 80 km curve of Fig. S-3, we observe that reduction to 0.32 occurs at 1.5 burst heights from ground zero or 1.5 x 80 = 120 km. The radius of the circle on which 10 cal/cm^2 is received the first second after detonation is thus 120 km.

OPERATIONAL IMPLICATIONS

Characteristics of the upper atmosphere above 50 km explored in this report rule out the possibility of maximizing the radius of destruction of a giant weapon by detonating the weapon at above-the-atmosphere heights of greater than about 80 km.

This altitude limitation has several immediate implications. One is that for detonations above 80 km, only that x-ray radiation directed "toward the ground" has any significance in creating ground effects. "Toward the ground" is shown to mean, in this study, radiation directed within roughly 45 degrees of the vertical. The initial x-ray radiation from the explosion is propagated in all directions. Those x-rays directed upward, away from the ground, will pass without significant hindrance into outer space. The rays within the roughly 45 degree cone directed downward, in an above-the-atmosphere detonation will produce an extended fire-pancake at the 80 to 90 km level. As a result, less than one-quarter*of the explosion energy is available for heating air which can then reradiate its energy to the ground. Thus, a weapon detonated slightly below 80 km is more than four times as effective as the same weapon detonated at a height slightly above 80 km. Further increases in altitude beyond 80 km give a further decrease in thermal efficiency, but at a rate of decrease far less than that which occurs near 80 km.

Another important implication of the fireball ceiling is the existence of a maximum ground range which is independent of yield. This limitation is the result of the curvature of the earth and is illustrated in Fig. S-4. The maximum radius of the area on the ground that the fireball of a weapon exploded at a given detonation height can "see" is given by its extreme ground range. At 80 km the maximum ground range is 1000 km. For burst heights above 80 km, the maximum possible ground range is 1000 km plus the radius of the fire pancake (which is about h-80 km).

The above facts alone present problems for an attacker who wishes to maximize both the amount of heat delivered at the ground and the area over which damaging amounts of heat (say 5-10 cal/cm^2, within 1 to

---

* One-quarter was taken throughout this study even though the geometric value is nearer 15%.

LOCAL ELEVATION ANGLE

CENTER OF FIREBALL

LOCAL HORIZONTAL

GROUND ZERO

EXTREME LIMIT OF GROUND RANGE (E = 0)

90°

RADIUS OF EARTH

θ
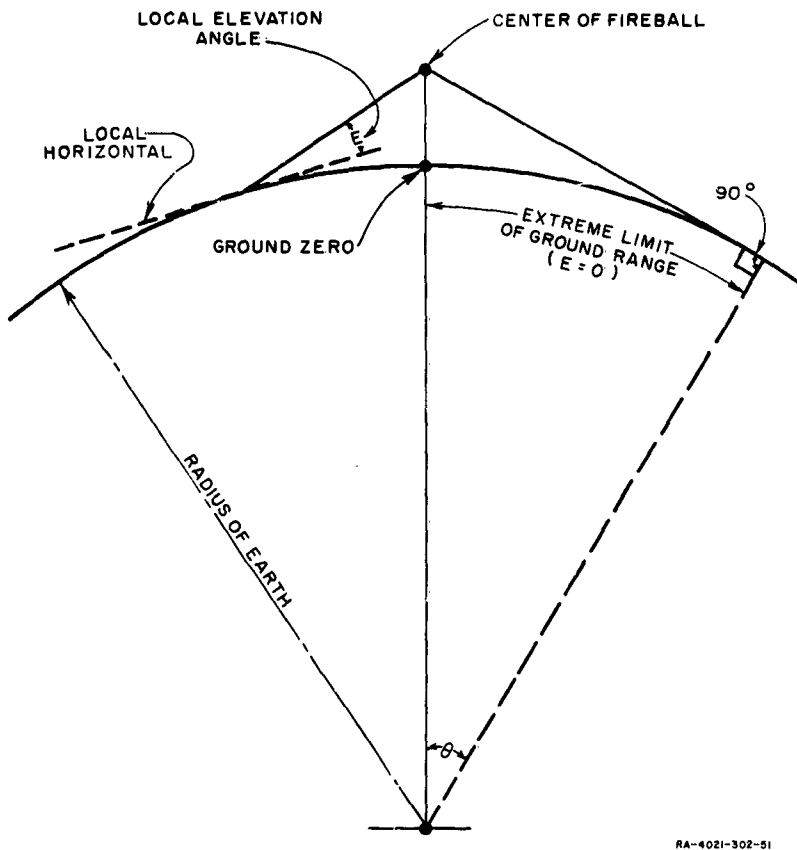
RA-4021-302-51

FIG. S-4 GROUND RANGE LIMITS OF THE THERMAL EFFECTS FROM NUCLEAR DETONATIONS CAUSED BY THE CURVATURE OF THE EARTH

10 sec, enough to set dry materials such as paper or fallen leaves afire)
are received. The higher he goes, the "farther the bomb can see" incen-
diary targets, but the smaller the energy per unit area it delivers any-
where within the circle of potential influence.

Another fact noted in the study is that the time during which the
x-ray energy of a detonation is reradiated to the ground after being
absorbed by air molecules tends to grow longer as the altitude of the
explosion.is increased. This effect further reduces the fire ignition
potential. In this connection it is well to remember that the sun
delivers 700 cal/cm^2 during one full July day at the latitude of Boston.
The fact that such levels are delivered at the rate of only $1/30$ cal/cm^2-sec
is the reason why such energy fluxes are not capable of ignition.

The study has noted that the efficiency of atmospheric transmission
of these wavelengths is between 75% and 80% for vertical rays (which
have the shortest possible path to the ground) but drops as low as 35%
at a low angle to the horizontal, 11 degrees, and drops still further
at elevation angles below 11 degrees. Thus, the heat effects at the
extreme ground range from a high altitude nuclear explosion would in-
evitably be less even without the consideration of the "floor and ceiling"
effect at 80 km, and even without the inevitable inverse square law
losses at great ranges.

The study has assumed a 100% transparent atmosphere. The presence
of clouds, fog, haze, dust, high humidity, etc., would decrease even
further the effects of an upper atmosphere (50-80 km) or above-the-
atmosphere (>80 km) detonation, especially at long ranges. A sequel
study to this one reports an investigation of the effects of the presence
of these factors.

Another consideration "neglected" in this study was that of shadowing.
At small elevation angles, shadows of even small objects are quite long,
and thus surfaces behind the objects are protected. The study also
assumed that all surfaces in range were "tilted" to face the incoming
rays directly, which would not be true in actuality. However, in a
given target region numerous optimally oriented surfaces exist and they
would serve as ignition points.

The implications of this study seem to rule out the use of orbiting weapons of sizes feasible in the coming decade or so (100 to 1000 mt) to maximize the area covered by thermonuclear heat effects. Because of atmospheric drag and other considerations, any large object would have to be orbited higher than 500 km to have a lifetime longer than a few days and to assure reasonable control of the weapon. The higher the detonation, the greater the direct losses of energy to space, and the longer the duration (for any given size weapon) of the pancake effects at the 80-km height. Of course, a weapon stored in a stable high orbit could be brought to lower altitudes by retro-rocket techniques, but then the area "seen" by the weapon at its detonation height would correspondingly shrink. To deliver sufficient heat to the ground from a detonation at orbital altitudes to "burn out several Western states" as has been speculated by some observers of weapons development, would require warheads much larger than is probably feasible for this decade. To launch these super-warheads and place them in stable orbits would require sophisticated rocket hardware of a size and expense comparable to those required for large, manned, lunar expeditions.

I   INTRODUCTION

A study of the fire-starting potential of nuclear weapons revealed much diversity among the current estimates of energy pulses from high-yield (greater than 1 mt) weapons detonated at high altitudes (above 50 km). To resolve this diversity, the problem was reinvestigated. This report explores the basic physical laws that will govern energy transfer from pulsed point sources at temperatures near 10^7 ^{0}K, the temperature assumed characteristic of nuclear weapons in Ref. 1.

Much is already known and published regarding energy transfer in the form of shock waves and thermal radiation for bursts at altitudes to 30 km.[1] Above 30 km, shock effects diminish rapidly so that at altitudes above 50 km they are not significant, leaving thermal radiation as the chief mechanism of energy transfer.

In this report we consider only altitudes above 50 km to explore theoretically the radiative energy transfer processes free of major shock wave effects. Experimental data in this altitude region is sparse, coming only from the Teak (77 km) and Orange (43 km) shots.[1] Thus the theoretical model developed here should be roughly consistent with the general observations reported in Ref. 1 on Teak and Orange.

All calculations performed here ignore possible attenuation of the thermal radiation by atmospheric haze, fog, or clouds. Since no possibility exists of cloud layers above 50 km to enhance by reflection the energy arriving at the ground, the results presented here are definitely upper limits, well above the energy fluxes which would be obtained on a day of exceptional clarity (visibility of 150 km) and low humidity.

The main features of nuclear detonations above 50 km which affect radiant energy transfer are:

1. The instantaneous emission at the time zero of a pulse of x-ray photons representing up to 4/5 the yield, with mean energy in the region of 1-10 kev.

2. When the burst occurs at an altitude between 50 and 80 km, the absorption of most of the energy of the x-ray photon pulse by a roughly spherical volume of the surrounding air having a radius ~1 mean free path for 1- to 10-kev x-rays.

3. The transfer of the absorbed energy into adjacent cold air by radiative transfer until a roughly uniform temperature of $20,000^\circ K$ is reached.

4. Radiative cooling of the fireball from $20,000^\circ K$ to $\sim 5000^\circ K$ with a substantial fraction of the radiated energy reaching the earth's surface.

5. Cessation of radiant emission as a major cooling mode below $5000^\circ K$.

6. The rapid change from a nearly spherical fireball to one of pancake shape as burst height is increased beyond 80 km, the level of the pancake remaining always near 80-km altitude.

7. The loss of more than $3/4$ the total x-ray energy for all detonations above 80-90 km, because of radiation into space.

In this study it has been convenient to differentiate between two altitude regions. One is the 50-80 km region where fireballs are roughly spherical -- called the upper-atmosphere. The second is the region above 80 km which has been designated above-the-atmosphere. Thus above-the-atmosphere detonations (AA) and upper-atmosphere detonations (UA) will be more or less separately treated in this development of the theoretical model.

In Section II the details of the initial energy deposition by x-ray absorption for UA and AA detonations are treated.

Section III describes the radiating properties of hot air, under the assumption of thermal equilibrium.

Section IV gives a picture of the relative disposition of the radiant energy into three chief energy bands: (1) the O_2 absorption band, (2) the ozone absorption band, and (3) the atmospheric transparency band.

Section V deals with geometrical factors which influence the distribution of the energy relative to ground zero (the point on the ground directly below the burst point).

In Section VI are given general curves for calculating energy received at the ground as a function of yield and detonation height. Also given are effects circle radius-altitude profiles for three different yields, the effects circles being centered about ground zero and along whose perimeters some fixed energy per unit area is received.

2

II. ABSORPTION OF BLACK-BODY X-RAY SPECTRA BY AIR

General Discussion

In the energy range from 100 ev to 20 kev the x-ray mass absorption coefficient of air is well approximated by

$$\mu_{x\text{-ray}} = \frac{4 \times 10^3}{E^3} \ cm^2/gm \tag{II-1}$$

where E is the incident energy in kev.

In addition the atmospheric density as a function of altitude above the earth's surface may be approximated by

$$\rho = 1.36 \times 10^{-10} \ \exp(-Z/28) gm/cm^3, 147 < Z < 320$$
$$= 1.225 \times 10^{-3} \ \exp(-Z/7) gm/cm^3 \ Z < 147 \tag{II-2}$$

where Z is the altitude in km. In Fig. 1, this approximation is compared with the ARDC model atmosphere.

For a given x-ray spectrum F(E), the energy intensity I(X) transmitted by an absorber of thickness X is given by

$$I(X) = I_0 \int_0^\infty F(E) \exp(-\mu(E)X) dE \tag{II-3}$$

A black-body source of absolute temperature T_x emits radiation with the energy distribution

$$F(E) = \frac{15}{(\pi k T_x)^4} \frac{E^3}{[\exp(E/kT_x)-1]} \tag{II-4}$$

so that Eq.(II-3) becomes

$$I(T_x X) = I_0 \int_0^\infty \frac{15}{\pi^4} \frac{u^3}{[\exp(u)-1]} \exp(-\mu[ukT_x]X) du \tag{II-5}$$

where $u = E/kT_x$.

The quantity $I(T_x, X)$ is plotted vs. absorber thickness in Fig. 2 from a paper by Kerr.[2]

3
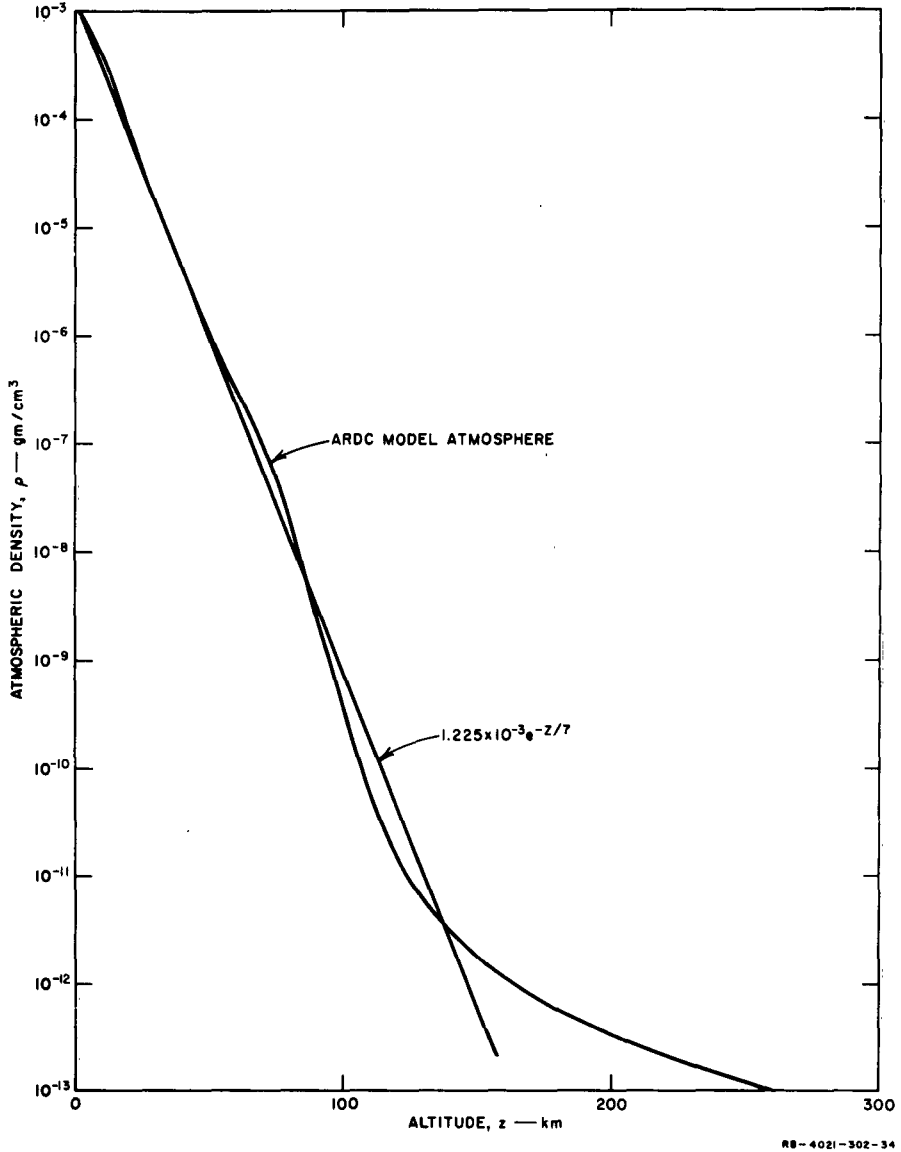
FIG. 1 ATMOSPHERIC DENSITY vs. ALTITUDE FOR TWO MODEL ATMOSPHERES

4
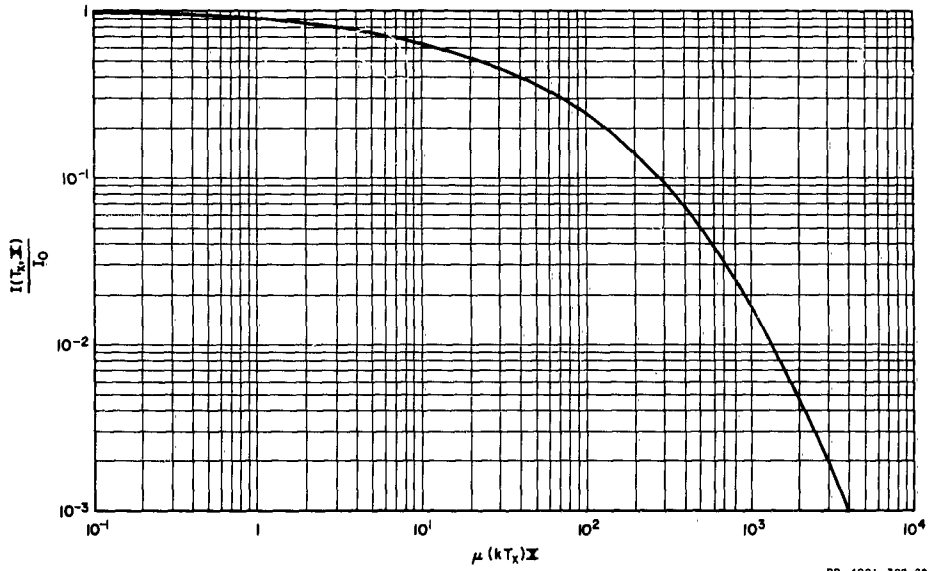
FIG. 2 X-RAY TRANSMISSION vs. ABSORBER THICKNESS FOR AN INCIDENT BLACK-BODY
        SOURCE (Absorber Thickness is Given in Terms of the Absorption Coefficient for
        Monoenergetic X-rays of Energy kT_x)

5

For atmospheric attenuation, X represents the mass surface density, $P(\vec{b},\vec{r})$, where the mass surface density from the burst point $\vec{b}(0,0,h)$ to the point of interest $\vec{r}(r,\theta,Z)$ is given by

$$P(\vec{b},\vec{r}) = \int_0^1 \rho(Z+x(h-Z)) \mid \vec{b}-\vec{r} \mid dx \quad gm/cm^2 \qquad (II-6)$$

where x is the fractional distance from $\vec{r}$ to $\vec{b}$.

Detonation Above-The-Atmosphere

For an above-the-atmosphere detonation we are most concerned with those x-rays coming from a detonation height h > 125 km straight down to the denser air at a height Z < 100 km, so that

$$P(\vec{b},\vec{r}) = P(h,Z) \approx P(Z) = 7 \times 10^5 \, \rho(Z) \quad gm/cm^2 \qquad (II-7)$$

which holds as long as Z < 147 km, $(h-Z) > 25$ km, and the path from $\vec{b}$ to $\vec{r}$ is along the vertical. For a nonvertical path, P(Z) above must be multiplied by the secant of the angle that the nonvertical direction makes with the vertical.

Eq.(II-5) thus becomes in the case of a vertical path as described above:

$$\frac{I(T_{x_1},Z)}{I_o} = \int_0^\infty \frac{15}{\pi^4} \frac{u^3}{[\exp(u)-1]} \exp[\frac{-\mu(kT_x)}{u^3} P(Z)]du \qquad (II-8)$$

Detonation in the Upper-Atmosphere

For an upper-atmosphere shot, the x-rays are absorbed in the atmospheric gases immediately about the detonation point. From the plot of $I(T_x,X)/I_o$ vs. X given in Fig. 2 and Eq.(II-1) we see that $(1-1/e)$ of the energy is absorbed in a distance $L_{1/e}$ given by

$$L_{1/e} = \frac{10(kT_x)^3}{(\rho/\rho_o)} \quad cm \qquad (II-9)$$

where $\rho_o = 1.293 \, gm/cm^3$ (STP) and (kT_x) is in kev.

Since it follows from Eq. (II-7) that above a given altitude there is only the equivalent of one scale height (7 km) of air at the density corresponding to that altitude, it is seen that as $L_{1/e}$ becomes comparable with a scale height, the x-rays from the device leaving in the upward direction are no longer significantly absorbed by the atmosphere. Their energy is therefore "lost to space". Thus it is seen that the condition

$$\frac{\rho(Z)}{\rho_o} < 1.43\times10^{-5} \ (kT_x)^3 \qquad\qquad (II-10)$$

essentially determines the height Z above which the x-rays from the device are no longer absorbed in the immediate vicinity of the detonation point. Altitudes below this height have been defined as the upper-atmosphere; and altitudes above this height have been defined as above-the-atmosphere, in which x-rays from the device are absorbed only in the denser layers of air lying below the detonation point. For an initial incident black-body temperature (kT_x) of 1 kev, $\rho(Z)/\rho_o = 1.43\times10^{-5}$, determining Z = 81 km as the height below which most of the x-ray energy is absorbed within a scale height of the detonation points, and above which only those x-rays directed towards the earth are absorbed.

Temperature to Which the Absorbed X-ray Energy Heats the Air

The internal energy of heated air[3] may be approximated by

$$E_I = 3.5\times10^2 \ T^{\frac{3}{2}}(\rho/\rho_o)^{0.9} \text{ergs/cm}^3 \ (T>10^4 \ ^\circ K) \qquad\qquad (II-11)$$

$$E_I = 10T^2(\rho/\rho_o) \text{ergs/cm}^3 \ (10^3<T<10^4 \ ^\circ K \text{ and} \atop (\rho/\rho_o)<10^{-3}) \qquad\qquad (II-12)$$

where T is the temperature of the heated air volume in $^\circ K$ (see Fig. 3).

For an upper atmosphere detonation, $(1-1/e)$ of the x-ray energy of the detonation will be deposited within an air mass whose volume is roughly given by $\frac{4}{3}\pi \ L_{1/e}^3$, so that the average temperature in this volume (the x-ray fireball) will be given by
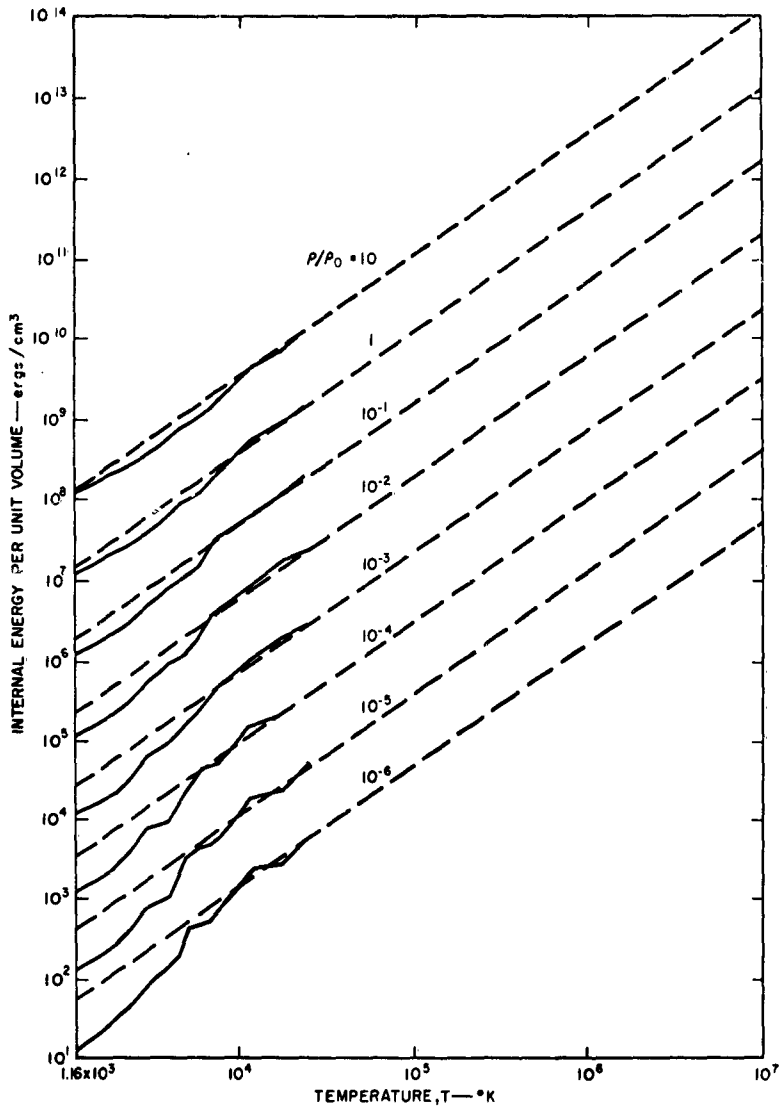
FIG. 3   INTERNAL ENERGY OF AIR (after Gilmore, Ref. 3)

8

$$3.5 \times 10^2 \; T_{RR_o}^{\frac{3}{2}} \; (\rho/\rho_o)^{0.9} \; \tfrac{4}{3}\pi \; L_{1/e}^3 = (1-1/e)4.18 \times 10^{22} Y \; \text{ergs/cm}^3 \qquad \text{(II-13)}$$

$$T_{RR_o} = \frac{6.8 \times 10^{10}}{(kT_x)^6} \; (\rho/\rho_o)^{1.4} Y^{\frac{2}{3}} \; {}^\circ K \quad (T > 10^4 \; {}^\circ K) \qquad \text{(II-14)}$$

where Y is the yield in mt (megatons of TNT energy equivalent --
4×10^{22} ergs/mt) of the detonation and T_{RR_o} denotes the initial temperature
of the irradiated air volume after x-ray energy deposition. For $\rho/\rho_o =$
10^{-5} (corresponding to a detonation height, h, of 83 km) and an incident
black-body temperature of 1 kev (kT), we see that any yield over 5 mt
will heat the surrounding air to a temperature, T_{RR_o}, of at least
$2 \times 10^4 \; {}^\circ K$. In the next section it will be shown how such superheated
air radiatively cools down from these temperatures. For any yield at
any burst height, a practical question is how much of the heat surrendered
in the cooling process reaches the ground.

For the absorption of energy by the atmosphere for AA detonations,
we must consider the differential deposition of energy at each altitude
as x-rays proceed toward the earth. The temperature at a given point
directly above ground zero is determined by equating the internal energy
of the air, E_I (known as a function of temperature) at a given altitude
with the x-ray energy deposited at that altitude, so that there follows

$$\begin{aligned} E_I &= \frac{dI(T_x, P(Z))}{dZ} \; \text{ergs/cm}^3 \\ &= I_o \mu(kT_x) P(Z) \int \frac{15}{\pi^4} \frac{\exp\left[\frac{-\mu(kT_x)}{u^3} P(Z)\right]}{\exp(u)-1} \, du \end{aligned} \qquad \text{(II-15)}$$

In Fig. 4 is plotted

$$A(T_x, P(Z)) = \frac{1}{I_o \rho(Z)\mu(kT_x)} \frac{dI(T_x, P(Z))}{dZ} \qquad \text{(II-16)}$$

vs. absorber thickness (mass surface density) as obtained from a differ-
entiation of Eq.(II-8) by graphical and numerical methods.

9
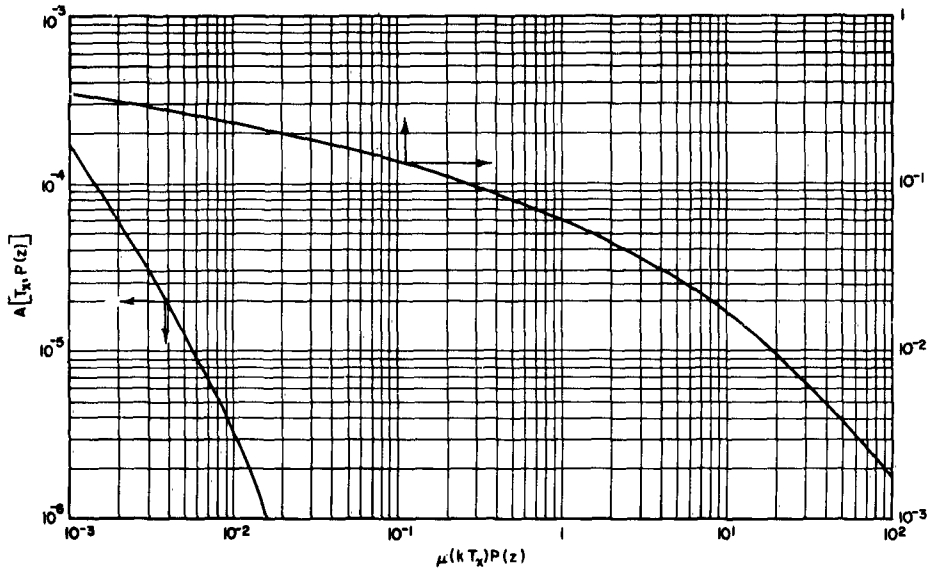
FIG. 4   DERIVATIVE OF X-RAY TRANSMISSION WITH RESPECT TO
ABSORBER THICKNESS vs. ABSORBER THICKNESS

RB-4021-302-45

10

With the stated assumption that 4/5 of the initial energy of the detonation appears as x-rays, it follows that

$$T_{RR_0}^2 = \frac{1.38 \times 10^{11} \; A(T_x, P(Z))Y}{(h-Z)^2 \; (kT_x)^3} \quad (10^3 \; {}^{\circ}K < T < 10^4 \; {}^{\circ}K) \qquad (II-17)$$

Similarly,

$$T_{RR_0}^{\frac{3}{2}} = \frac{1.20 \times 10^9 \; A(T_x, P(Z))Y}{(h-Z)^2 \; (kT_x)^3} \; (\rho/10^{-8})^{0.1} \quad (T > 10^4 \; {}^{\circ}K) \qquad (II-18)$$

where $(h-Z)$ is in km, (kT_x) is in kev, and T_{RR_0} is in ${}^{\circ}K$.

From Eqs. (II-17) and (II-18) it is seen that the yield Y required to heat air at a given density (and therefore at a given altitude) to a required temperature T_{RR_0} goes as $[(kT_x)^3/A(T_x, P(Z)]$.

In Fig. 5 this quantity is plotted at densities $\rho = 10^{-7}$, 10^{-8}, and 10^{-9} grams/cm^3, thus determining the initial black-body temperature which will be most effective in heating air at these respective densities.

It is seen from Fig. 5 that air at a density of 10^{-9} grams/cm^3 is most effectively heated by an AA detonation in which the incident black-body spectrum is described by $(kT_x) = 0.6$ kev; at 10^{-8}, by a spectrum described by $(kT_x) = 1.25$ kev; and at 10^{-7}, by a spectrum described by $(kT_x) = 2.4$ kev; and that the amount of energy required to heat any given layer to a specified temperature is roughly proportional to the air density at that layer. In addition, most of the energy absorbed by the atmosphere in an AA detonation will be absorbed within a couple of scale heights of the altitude optimally heated by a black-body x-ray spectrum of temperature T_x.
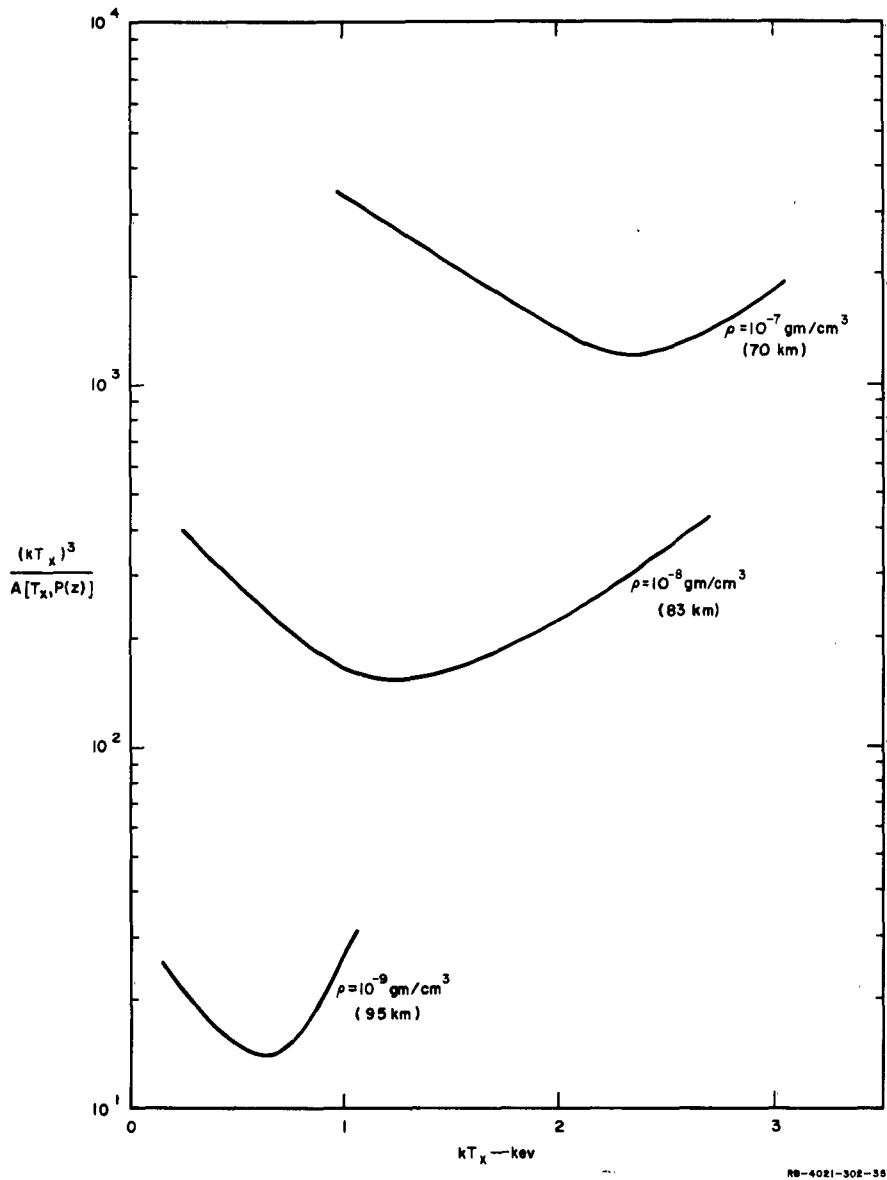
11

FIG. 5 A QUANTITY PROPORTIONAL TO THE YIELD REQUIRED TO HEAT AIR TO A GIVEN
TEMPERATURE vs. THE BLACK-BODY TEMPERATURE OF THE INCIDENT
SPECTRUM FOR AIR DENSITIES OF 10^{-7}, 10^{-8}, AND 10^{-9} gm/cm^3

III   RERADIATION OF THE ABSORBED INITIAL X-RAY ENERGY BY HEATED AIR

In this section it will be assumed that the air heated by x-ray deposition reradiates its energy as if it were a black-body. The emissivity (and hence the opacity) of this black-body is assumed to be determined by the composition of the air at whatever temperature corresponds to thermodynamic equilibrium.

Following Chandrasekhar,[4] the equation of radiative transfer for an atmosphere in thermodynamic equilibrium is given by:

$$\frac{dN_\upsilon}{ds} = \mu'_\upsilon (B_\upsilon - N_\upsilon) \text{ergs-cm}^{-3}\text{-sec}^{-1}(\text{unit frequency in sec}^{-1})^{-1}\text{sterad}^{-1}$$

$$(\text{III-1})$$

where N_υ is the emitted energy flux per unit solid angle per unit projected area, per unit frequency band and s is distance in cm. (By projected area is meant the quantity $dA\cos\varphi$ where dA is the area of an element of the emitting surface and φ is the angle between the direction or propagation and the normal to the emitting surface.) B_υ is the black-body spectrum given as a function of the frequency υ by

$$B_\upsilon = \frac{2h\upsilon^3}{c^2}(\exp(h\upsilon/kT)-1)^{-1}\text{ergs-cm}^2\text{sec}^{-1}(\text{unit frequency in sec}^{-1})^{-1}\text{sterad}^{-1}$$

$$(\text{III-2})$$

μ'_υ is the reduced absorption coefficient of air (cm^{-1}) corrected for induced emission, and is given by

$$\mu'_\upsilon = \mu_\upsilon(Z,T)(1-\exp(-h\upsilon/kT)) \qquad (\text{III-3})$$

μ_υ is, in general, a function of both the temperature and density of the atmosphere.

In the upper atmosphere (below about 80 km) the reradiating volume surrounding the detonation point is approximately spherical in shape (flattened at the bottom since the denser air below decreases the x-ray mean free path; and elongated at the top, since the rarer air above increases the x-ray mean free path). In AA bursts the reradiating volume

can be considered, to a first approximation, to be a plane circular layer
a few scale heights in depth.

To solve Eq. (III-1) we integrate from a point where the intensity in
a required direction equals zero to the outer surface of the radiating
volume. For UA bursts, the net reradiated intensity in any given direc-
tion equals zero at the detonation point; for AA bursts, the downward
reradiated intensity equals zero at the top surface of the reradiating
layer (neglecting the radiation from the rarer, and therefore less
effective radiating volumes closer to the detonation point.) Thus we
can solve Eq. (III-1) to obtain

$$N_\nu(s) = \int_0^s \mu'_\nu B_\nu \exp(-\mu'_\nu(s-s'))ds' + I(o)\exp(-\mu'_\nu s) \qquad (III-4)$$

where we have assumed reradiating bodies of constant temperature and
density. In this expression, $I(o)$ is the incident energy flux in the
required direction at $s = 0$ (under the above assumptions, $I(o) = 0$).
The integral term sums the contributions to the directed emitted energy
flux from the radiating volumes between $s'= 0$ and the position s,
correcting for absorption between the radiating volumes and s.

For all but the lowest black-body photon energies, which will be
absorbed by water and other infrared absorbers in the air and so will
not affect the radiation observed on the ground, $(1-\exp(-h\nu/kT)) = 1$,
and therefore $\mu'_\nu = \mu_\nu$. The radiation coming from a heated region of
dimension s will thus be given by

$$N_\nu(s) = (1-\exp(-\mu_\nu s))B_\nu \simeq \mu_\nu sB_\nu \qquad (III-5)$$

for any $\mu_\nu s$ much less than 1, i.e., a gas which is relatively transparent
to its own radiation. In both UA and AA detonations, the absorption
coefficient μ_ν is such that the reradiating air mass is opaque to the
incoming x-rays but transparent to its own longer wavelength reradiation.

For UA detonations, s in Eq. (III-5) is replaced by R, the mean
radius of the reradiating fireball. In AA detonations, s in Eq. (III-5)
is replaced by d, the depth of the effective reradiating layer. To

14

obtain the rate at which energy is radiated across a given surface we must integrate Eq. (III-5) over all frequencies and over all solid angles. For a perfectly diffuse surface, the integration over all solid angles merely introduces a factor of π so that the result is given by

$$I(s) = \pi \bar{\mu} \ s(\frac{\sigma T^4}{\pi}) \text{ ergs-cm}^2 \ \text{sec}^{-1} \qquad (III-6)$$

$$= \bar{\mu} s \sigma T^4$$

where $I(s)$ is the total amount of radiant energy crossing the surface element dA of the radiating surface at s, per unit area per unit time; $\sigma = 2\pi^5 k^4/15c^2 h^3$ is the radiation constant and is equal to 5.67×10^{-5} ergs/(cm^2 sec ($^\circ$K)^4) and

$$\bar{\mu} = \frac{15}{\pi^4} \int \mu_\nu \ u^3 \ \exp(-u) du \ \text{cm}^{-1} \qquad (III-7)$$

is the mean absorption coefficient over the Planck distribution.

A more convenient quantity to work with is $d\mathcal{E}/dt$, the energy radiation rate per cubic centimeter of radiating volume, which is obtained from Eq. (III-6) by multiplying by the radiating area and dividing by the volume, so that

$$\frac{d\mathcal{E}}{dt} = \frac{\bar{\mu} s A_R}{V} \ \sigma T^4 \ \text{ergs cm}^{-3} \ \text{sec}^{-1} \qquad (III-8)$$

For UA bursts with a radiating fireball, $A_R = 4\pi R^2$, $V = \frac{4}{3}\pi R^3$, $S = R$, and Eq. (III-8) becomes

$$\frac{d\mathcal{E}_{UA}}{dt} = 3\bar{\mu}\sigma T^4 \ \text{ergs cm}^{-3} \ \text{sec}^{-1} \qquad (III-9)$$

For AA bursts with a thin reradiating layer, $A_R = 2A$, $V = Ad$, $s = d$, and, neglecting the radiation from the edges of the layer, there follows

$$\frac{d\mathcal{E}_{AA}}{dt} = 2\bar{\mu}\sigma T^4 \ \text{ergs cm}^{-3} \ \text{sec}^{-1} \qquad (III-10)$$

The equilibrium composition of air to 2.4×10^4 °K is given in Ref.3; with the aid of these results, the absorption coefficients for air have been computed by Meyerott, et al.[5] in the range 10^3 to 1.2×10^4 °K and by Armstrong et al.[6] in the range 2.2×10^4 to 22×10^4 °K. In particular Kivel and Bailey[7] have computed the Planck mean absorption coefficient and the volume emission rate for air in the range 10^3 to 1.8×10^4 °K. Their results for the energy radiated per second per cm^3 (volume emission rate by a thin planar sheet are given in Fig. 6. These results can be approximated by

$$\bar{\mu}\sigma T^4 = 4.1 \times 10^{11} (\rho/\rho_o)^{1.5} (\frac{T}{10^4})^9 \text{ergs-cm}^3 \text{ sec}^{-1}$$
$$(3 \times 10^3 < T < 1.5 \times 10^4 \text{ °K}) \tag{III-11}$$

$$\bar{\mu}\sigma T^4 = 5.0 \times 10^{15} (\rho/\rho_o)^2 \text{ergs-cm}^{-3} \text{ sec}^{-1}$$
$$(T > 1.5 \times 10^4 \text{ °K}) \tag{III-12}$$

Beyond 2.5×10^4 °K, $\bar{\mu}$ has very roughly a value of $10^2 (\rho/\rho_o)^2$ cm^{-1} (see Armstrong et al.[6]), so that the radiation rate again increases, with

$$\bar{\mu}\sigma T^4 = 5.7 \times 10^{-3} (\rho/\rho_o)^2 T^4 \text{ ergs-cm}^{-3} \text{ sec}^{-1} \quad (T > 2.5 \times 10^4 \text{ °K}) \tag{III-13}$$

This quantity is also plotted in Fig. 6.

The equilibrium temperature of the reradiating air mass as a function of time is then determined from the equation

$$\frac{d\mathcal{E}}{dt} = \frac{dE_I}{dt} \tag{III-14}$$

where E_I has been given in Eqs.(II-11) and (II-12). To solve this equation, the four regions: $3 \times 10^3 < T < 10^4$, $10^4 < T < 1.5 \times 10^4$, $1.5 \times 10^4 < T < 2.5 \times 10^4$, $T > 2.5 \times 10^4$ °K are considered separately, the results becoming:

$$T = \frac{T_{RR_o}}{[1 + 4 \times 10^{-28} f(\rho/10^{-8})^{0.5} T_{RR_o}{}^7 t]^{1/7}}, \quad (3000 < T < 10,000) \tag{III-15}$$
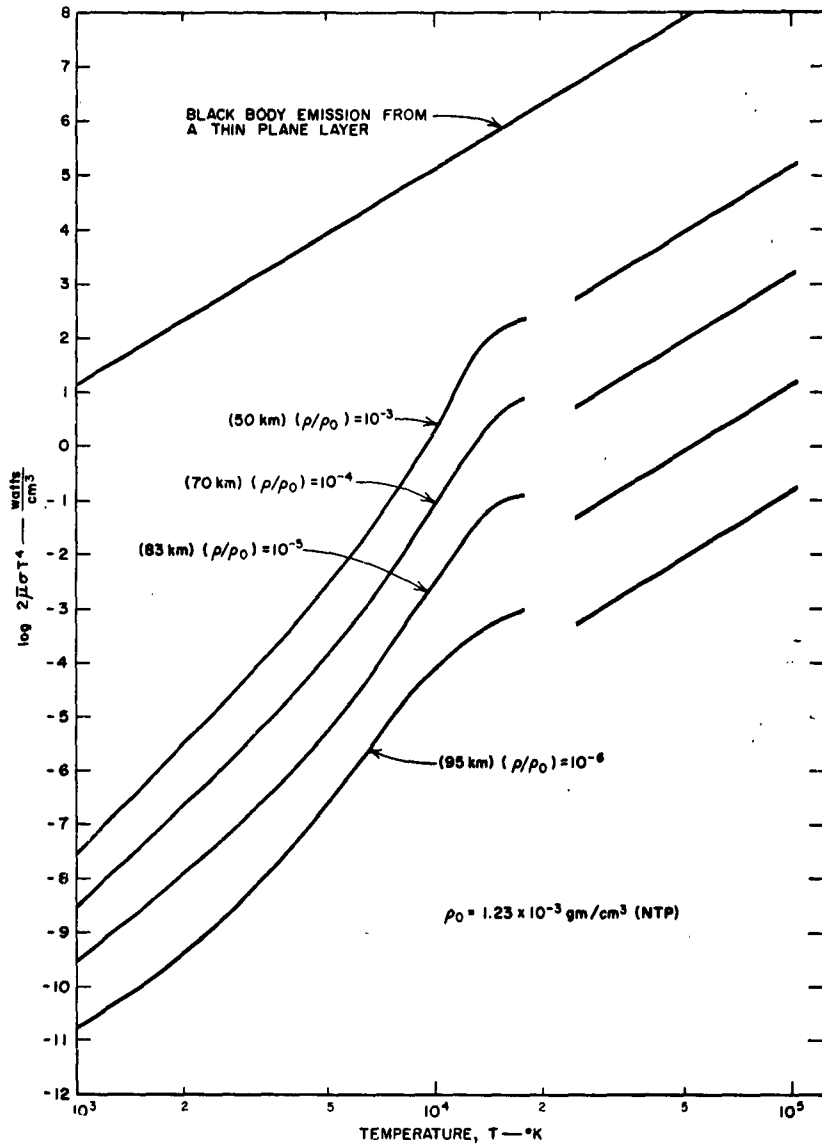
FIG. 6   TOTAL EMISSION FROM A PLANE THIN LAYER OF AIR AS A
FUNCTION OF TEMPERATURE

17

$$T = \frac{T_{RR_o}}{[1 + 5\times10^{-30}f(\rho/10^{-8})^{0.6}T_{RR_o}^{7.5}t]^{2/15}} \ , (10{,}000 < T < 15{,}000) \quad \text{(III-16)}$$

$$T = [T_{RR_o}^{3/2} - 3.5\times10^7 f(\rho/10^{-8})^{1.1}t]^{2/3}, (15{,}000 < T < 25{,}000) \quad \text{(III-17)}$$

$$T = \frac{T_{RR_o}}{[1 + 6.5\times10^{-11}f(\rho/10^{-8})^{1.1}T_{RR_o}^{5/2}t]^{2/5}} \ (T, T_{RR_o} > 25{,}000^\circ K) \quad \text{(III-18)}$$

where $f = 2$ for a thin radiating layer and $f = 3$ for a spherical radiator.
From Eq.(III-18) it is seen that it takes at most

$$t_1 = \frac{0.15}{f}(\rho/10^{-8})^{-1.1} \text{ sec} \quad \text{(III-19)}$$

for the reradiating air, however hot initially, to cool to 2.5×10^4 $^\circ K$.
Similarly, it takes

$$t_2 = \frac{0.060}{f}(\rho/10^{-8})^{-1.1} \text{ sec} \quad \text{(III-20)}$$

for the air to cool from 2.5×10^4 to 1.5×10^4 $^\circ K$;

$$t_3 = \frac{0.190}{f}(\rho/10^{-8})^{-0.6} \text{ sec} \quad \text{(III-21)}$$

to cool from 1.5×10^4 to 10^4 $^\circ K$; and

$$t_4 = \frac{0.25}{f}(\rho/10^{-8})^{-0.5}\left[(\frac{10^4}{T})^7 - 1\right] \text{ sec} \quad \text{(III-22)}$$

to cool from 10^4 to a temperature T greater than 3×10^3 $^\circ K$.
In Fig. 7 is plotted the temperature T vs ft (two or three times the time) for $\rho = 10^{-8}$ gm/cm^3 and an initial temperature T_{RR_o} greater than 2.5×10^4 $^\circ K$.
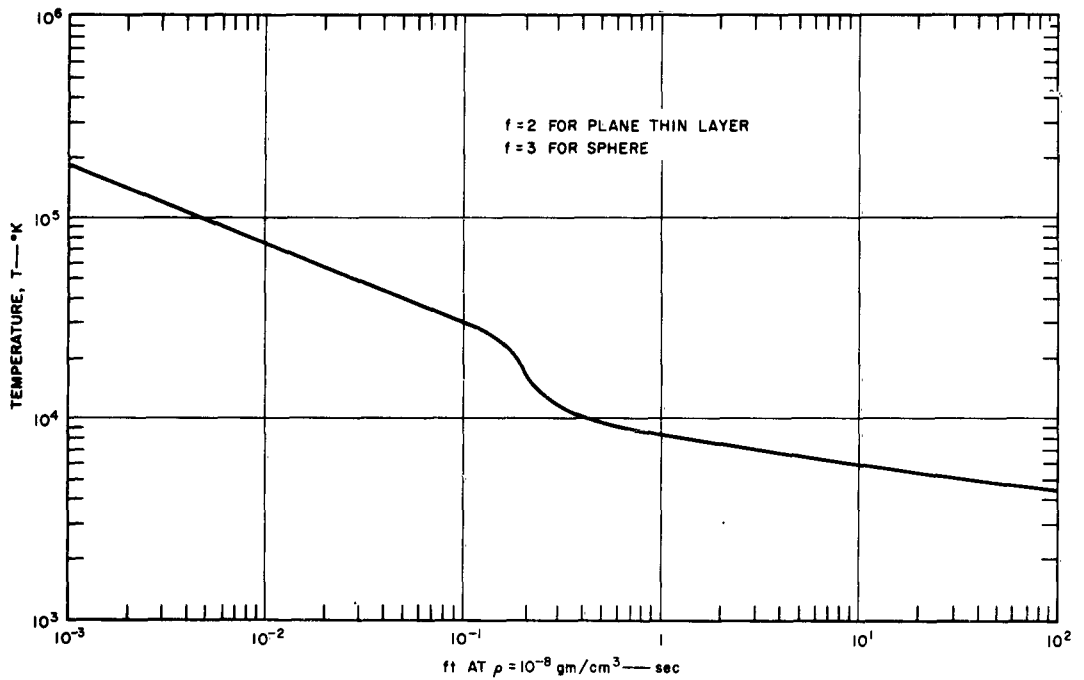
18

FIG. 7   TEMPERATURE vs. TIME FOR AIR AT A DENSITY OF 10^{-8} gm/cm^3
AND AN INITIAL TEMPERATURE GREATER THAN 2.5 $\times$ 10^4 °K

19

IV RERADIATION EFFICIENCIES INTO THE ATMOSPHERIC PASSBAND
AND TIME DEPENDENCE OF THE THERMAL RADIATION

Atmospheric Absorption Bands and Passbands

Because of infrared absorption by H_2O vapor and CO_2, and ultraviolet absorption by O_2 and O_3, the atmosphere is transparent to photon energies lying between, roughly, 0.65 and 4 ev. From 4 to 6 ev, radiation is absorbed by O_3, which is concentrated in the atmosphere between 20 and 40 km. Above 6 ev, radiation passing through the atmosphere is absorbed principally by O_2 but also by N_2.[8] The O_2 absorption coefficient for frequencies greater than 6 ev is so large, in fact, that even at 10^{-5} normal atmospheric density, any radiation of greater than 6 ev energy has an absorption mean free path of less than an atmospheric scale height (7 km).

In Fig. 8 is plotted the O_2 continuous absorption coefficient, k, at NTP, as taken from the Geophysical Handbook[8] and Weissler and Lee.[9] The peak at 1450A is due to Schumann dissociation of the O_2 molecule. Thus, it is seen that for $(\rho/\rho_o) = 10^{-5}$ and an air temperature of T, $\ell_{1/e}$, the mean free path for oxygen absorption, is given by

$$\ell_{1/e} = \frac{1}{(\rho/\rho_o)k(288/T)} = \frac{10^5}{k(288/T)} \text{ cm} \qquad \text{(IV-1)}$$

For $\ell_{1/e}$ less than 7×10^5 cm, an atmospheric scale height,

$$k > \frac{T}{2 \times 10^3} \text{ cm}^{-1} \qquad \text{(IV-2)}$$

so that even at the low density of 10^{-5} normal, the air immediately surrounding the reradiating volume will be able to absorb sufficient energy to heat itself to temperatures comparable with the original fireball and thus itself become part of the reradiating volume.

In Fig. 9 are plotted those fractions of energy of a black-body that lie within the O_2 and O_3 absorption bands, and also that fraction which lies within the atmospheric passband as a function of black-body temperature.[10] (Two assumed atmospheric passbands are shown, 0.65 to 4 ev and 0.65 to 3.6 ev.)
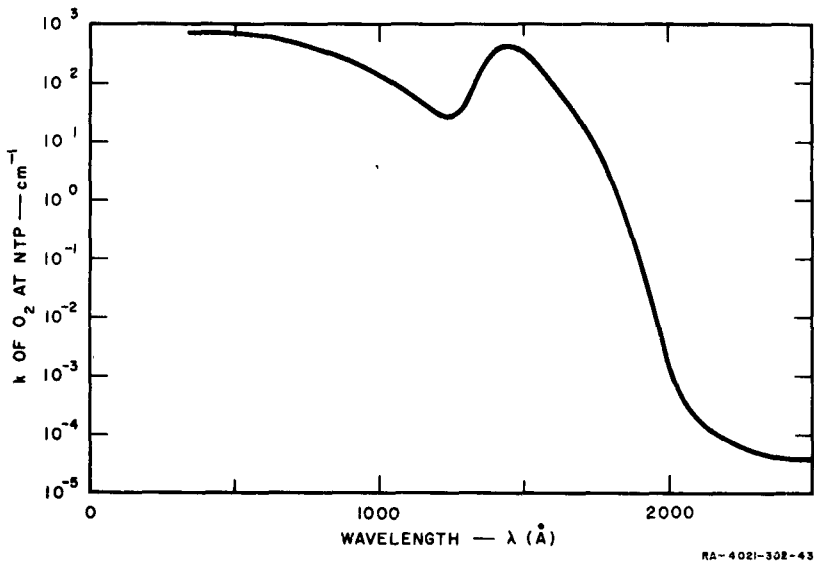
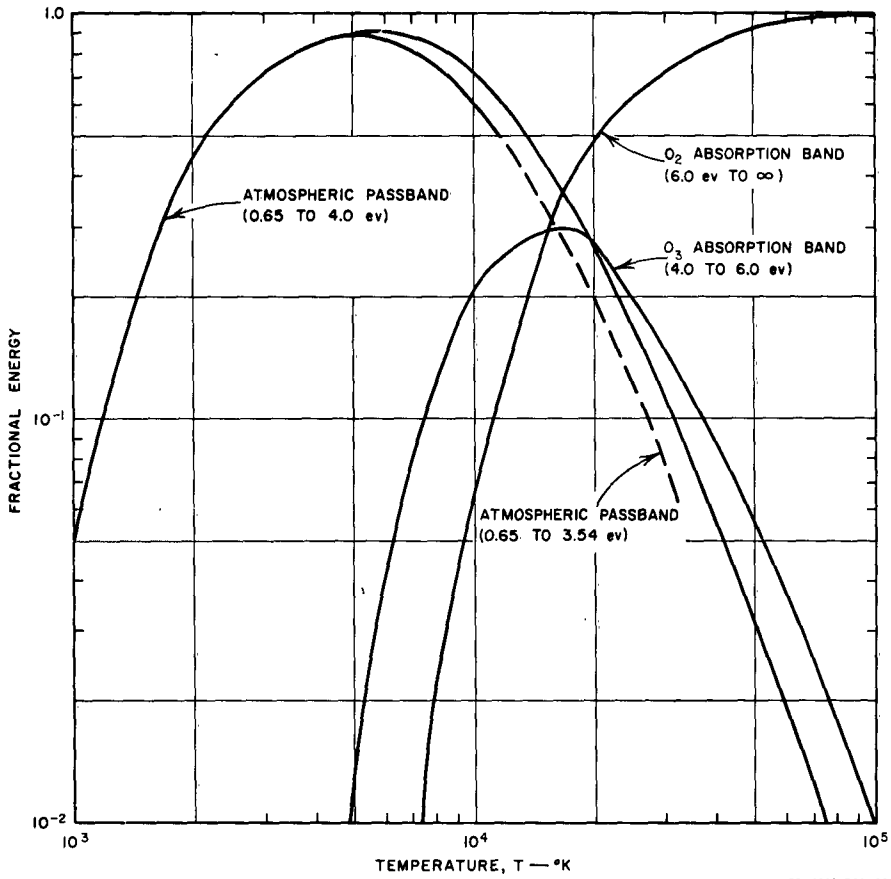FIG. 8 O_2 CONTINUOUS ABSORPTION COEFFICIENT (NTP)

FIG. 9   FRACTIONS OF BLACK-BODY ENERGY IN RELEVANT ENERGY RANGES
AS A FUNCTION OF BLACK-BODY TEMPERATURE

23

By inspection of this graph, it is seen that for black-body temperatures greater than 2×10^4 °K, >50% of the reradiated energy will be absorbed by the surrounding O_2 and therefore will increase the reradiating volume. Below 2×10^4 °K, >20% of the black-body energy will lie in the atmospheric passband and so will be transmitted to the ground. Thus, the radiation transfer process can be considered in two steps when the initial reradiation temperature, T_{RR_0}, is greater than 2×10^4 °K. In the first step, which will take place in about $0.05(\rho/10^{-8})^{-1.1}$ sec (see Eqs. (III-19) and (III-20)), the reradiating volume will cool down by expansion until it has an average temperature of about 2×10^4 °K; in the second step, this enlarged fireball will then cool down from 2×10^4 °K by reradiation into the atmospheric passband and thus to the ground. Since it has already been shown that in UA, any yield over 5 mt will result in an initial fireball temperature of greater than 2×10^4 °K, it follows that the energy reradiated into the atmosphere passband for UA for all yields greater than 5 mt, will be linear with the yield and will have an efficiency and time dependence roughly corresponding to a 2×10^4°K radiating volume at the detonation height h.

From Fig. 9 it is seen that the fraction of black-body energy in the atmospheric passband can be closely approximated by

$$\frac{\int_{0.65\ ev}^{4\ ev} \frac{E^3}{[\exp(E/kT)-1]}\ dE}{\int_{0}^{\infty} \frac{E^3}{[\exp(E/kT)-1]}\ dE} \approx 0.85 \quad (3000 < T < 10,000\text{°K}) \tag{IV-3}$$

$$\approx \frac{5.4 \times 10^6}{T^{1.7}} \quad (10,000 < T < 20,000\text{°K}) \tag{IV-4}$$

so that the energy reradiated into the atmospheric passband, E_R, as a function of T, for $T_{RR_0} = 2 \times 10^4$ °K, is given by

$$E_R(T_{RR_0} = 2 \times 10^4 \text{ °K}, T) = \int_{2 \times 10^4 \text{ °K}}^{T} \frac{5.4 \times 10^6}{T^{1.7}}\ dE_I(T) \tag{IV-5}$$

$$(T > 10^4 \text{ °K})$$

where E_I has been given in Eqs. (II-11) and (II-12). In Fig. 10 is plotted

$$\frac{E_R(T_{RR_o} = 2 \times 10^4 \ ^oK, \ T)}{E_I(T_{RR_o} = 2 \times 10^4 \ ^oK)}$$

as obtained from solving these above two equations. By reference to Fig. 7, this same quantity is plotted vs. (fT) at $\rho = 10^{-8}$ gm/cm^3, where it has been assumed that the initial fireball was much hotter than $2 \times 10^4 \ ^oK$, and that negligible atmospheric passband radiation occurred before this temperature of $2 \times 10^4 \ ^oK$ was attained. From Fig. 10 it is seen that roughly half of the energy of a $2 \times 10^4 \ ^oK$ UA fireball is reradiated in the atmospheric passband. Half of this half has radiated by the time the fireball has cooled to $10^4 \ ^oK$.

Upper-Atmosphere Bursts

    To obtain an estimate of the overall efficiency for the conversion of x-ray energy into energy reradiated in the atmospheric passband, there are two additional factors to be considered: (a) ozone absorption in the lower atmosphere, which will absorb about one-quarter of the reradiated energy of the fireball during the first-step cooling down process to $2 \times 10^4 \ ^oK$ (see Fig. 9); (b) energy which is absorbed too far from the center of the reradiating volume to heat the air to a reradiating temperature which includes both initial x-ray and also that reradiated energy greater than 6 ev reabsorbed by the surrounding O_2.

    This latter factor will account for another effective loss of about one-quarter of the original x-ray energy. Thus UA detonations will have an efficiency of about 25% for converting the original energy of the device into reradiation in the atmospheric passband. One-quarter is lost in O_3 absorption, one-quarter is ineffectively absorbed too far from the reradiating fireball to give those temperatures necessary for reradiation into the atmospheric passband, and of the remaining one-half, only one-half again is reradiated into the atmospheric passband. This
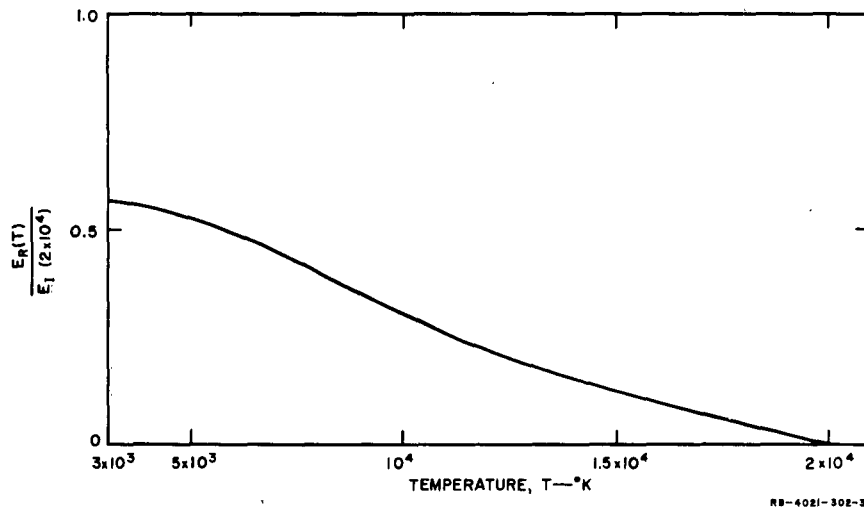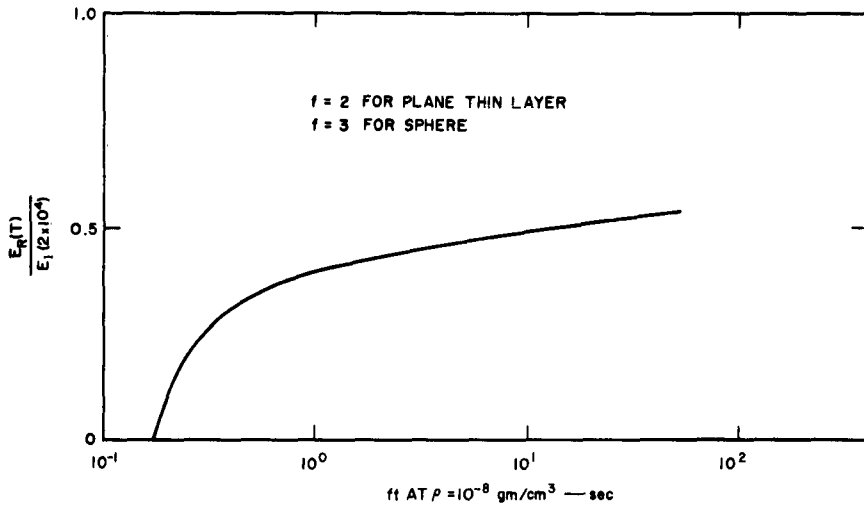
FIG. 10   FRACTIONAL ENERGY RADIATED FROM A 2×10^4 °K AIR MASS AS A FUNCTION OF TEMPERATURE AND AS A FUNCTION OF TIME FOR AN AIR DENSITY OF 10^{-8} gm/cm^3

26

result is in agreement with the efficiency for upper-atmosphere detonations of 25-35% as given in Ref. 1.

Consider now the time dependence of the radiation for the UA bursts. Radiation into the atmospheric passband will take place even during the first step of the cooling process in which the reradiating volume is cooling down to an average temperature of 2×10^4 °K, since even a black-body of temperature T greater than 2×10^4 °K has a finite amount of energy in the atmospheric passband. In addition, even at the earliest times the fireball will have outer sections at the more effective radiating temperatures (for the atmospheric passband) of less than 2×10^4 °K, since in reality the fireball is not uniform in temperature. These factors will produce radiation prior to $t_1 = 0.05(\rho/10^{-8})^{-1.1}$ sec, but will neither increase the total amount of energy reradiated nor affect the radiation rate for times when the fireball is more uniform in temperature. The overall result is thus that before $t' = t_1 + t_2 + t_3$ (at which time the fireball has a roughly uniform temperature of 10^4 °K) the net energy radiated is more constant with time than the above analysis would indicate.

From Fig. 10 it is seen that roughly 1/2 of the eventually radiated energy is radiated by the time a temperature of 10^4 °K is attained. After this time, it follows from Eqs. (III-11), (III-15), and (IV-3) that the power radiated into the atmospheric passband goes roughly as $t^{-9/7} = t^{-1.29}$. A rough estimate of the time behavior of the power radiated into the atmospheric passband can thus be made by considering that prior to $t' = t_1 + t_2 + t_3$, half of the total energy radiated is radiated as t^{-x} and that from t' to ∞ the remaining half is radiated as $t^{-9/7}$. To determine x, we equate

$$\int_{t'}^{\infty} t^{-9/7} \, dt = \int_{0}^{t'} t^{-x} \, dt \qquad \text{(IV-7)}$$

so that

$$\frac{t'^{(1-x)}}{1-x} = \frac{7}{2} t'^{-2/7} \qquad \text{(IV-8)}$$

27

x is plotted vs. t' in Fig. 11, where it is shown to be a very slowly varying function of t' with an average value of about 0.9. Also given in Fig. 11 is a plot of t' vs. z, thus giving x as a function of the altitude z.

The time dependence of the power radiated, dE_R/dt, is thus roughly given by

$$\frac{dE_R}{dt} \alpha\ t^{-x}\ (t<t')\ \text{(IV-9)}$$

$$\frac{dE_R}{dt} \alpha\ t^{-.97}\ (t>t')\ \text{(IV-10)}$$

where

$$t' = t_1+t_2+t_3 = 0.07\left[(\rho/10^{-8})^{-1.1}+(\rho/10^{-8})^{-0.6}\right]\ \ \ \ \ \text{(IV-11)}$$

is the time required for the fireball to cool to 10^4 °K (see Eqs.(III-19) to (III-21)) and x, as given in Fig. 11, is such that half of the total energy radiated is radiated prior to t', half antecedent to t'.

Above-the-Atmosphere Bursts

In AA detonations the reradiating volume is no longer roughly spherical, because the air immediately surrounding the detonation point is too rare to absorb enough of the energy of the device to be a significant radiator. From Eqs.(II-17) and (II-18) and also from Fig. 5, it is seen that for a device with a black-body x-ray temperature of approximately 1 kev, most of the energy will be absorbed between those altitudes for which the air density $\rho=10^{-7}$ gm/cm^3 and 10^{-9} gm/cm^3. In addition, for a density less than 10^{-9} gm/cm^3, Eqs.(III-19) to (III-22) predict a characteristic radiation time longer than 1 sec. Again from Eqs.(II-17) and (II-18) it is seen that the isothermal surfaces are given by

$$\frac{A(T_x,P(z_o))}{(h-z_o)^2} = \frac{A(T_x,P(z)\sec\theta)}{(h-z)^2}\ \ \ \ \ \ \ \ \ \ \ \ \ \ \ \text{(IV-12)}$$
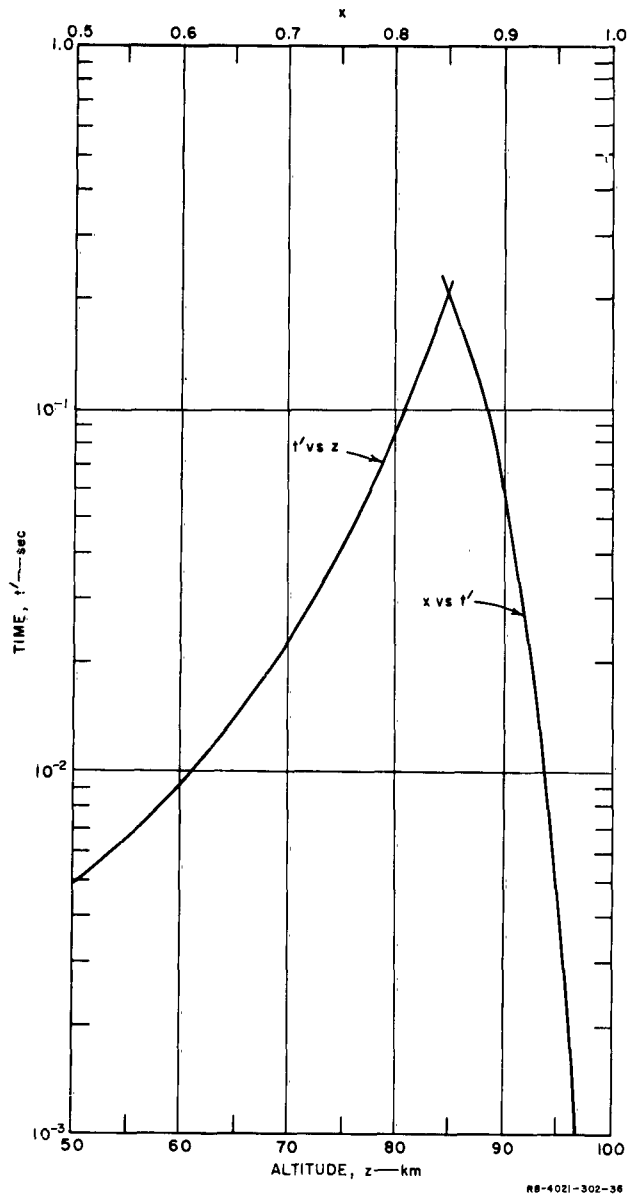
28

FIG. 11   A QUANTITY RELATED TO THE TIME DEPENDENCE AT EARLY TIMES OF THE
POWER RADIATED AS A FUNCTION OF ALTITUDE FOR DETONATIONS
IN THE UPPER ATMOSPHERE

29

where z_o is the height directly above ground zero of a point on a given isotherm, θ is the angle that the line from the detonation point to the required point on the isotherm makes with the local vertical, and z is the height of the point in question on the isotherm. In Fig. 12 are plotted isotherms determined from a graphical solution of Eq(IV-12) for two detonation heights. It is seen from this figure that the shape of the isotherm is such that approximately

$$\frac{\pi(h-z_o)^2}{4\pi(h-z_o)^2} = \frac{1}{4}$$

of the x-ray energy of the device goes into the heating of air which can then reradiate a significant amount of its energy into the atmospheric passband. A further loss of efficiency for AA bursts compared with UA bursts results from the fact that less than $4/5$ of the energy of the detonation goes into x-rays, and thus into heating of the lower lying air. For UA detonations, essentially all the energy of the detonation in the form of both x-rays and the kinetic energy of the fragments, is absorbed by the reradiating air immediately surrounding the detonation point.

To find the efficiency with which x-rays are absorbed and converted into atmospheric passband radiation for an AA detonation, the absorption and reradiation of the x-ray energy directly above ground zero is considered. From Eqs.(II-11) and (II-18), Fig. 13 is obtained, giving the temperature and internal energy distribution in the heated lower air layer for a detonation sufficiently high above the heated layers that the layer thickness is small compared with its distance from the detonation points.

The incident initial x-ray spectrum from the device is assumed to have a black-body temperature $(kT_x)=1.25$ kev, which has been shown to be the most effective temperature for heating the lower lying air at a density of 10^{-8} gm/cm^3 (see Fig. 5). Fig. 13 shows the temperature and energy distribution as a function of altitude directly below the burst point for an x-ray burst characterized by kT = 1.25 kev. Because of a

Within the figure:

$\frac{T}{T_0} = 1.5$ $\frac{T}{T_0} = 1$

BURST POINT AT h = 153km   X

$\frac{T}{T_0} = 2$

$\frac{T}{T_0} = 1.5$ $\frac{T}{T_0} = 2$

$\frac{T}{T_0} = 1$

97
90
83

(h − 83)

(h − 83)

SCALE: 1/2 DIVISION = 1 SCALE HEIGHT ≈ 7km

TO BURST POINT AT h = 293km
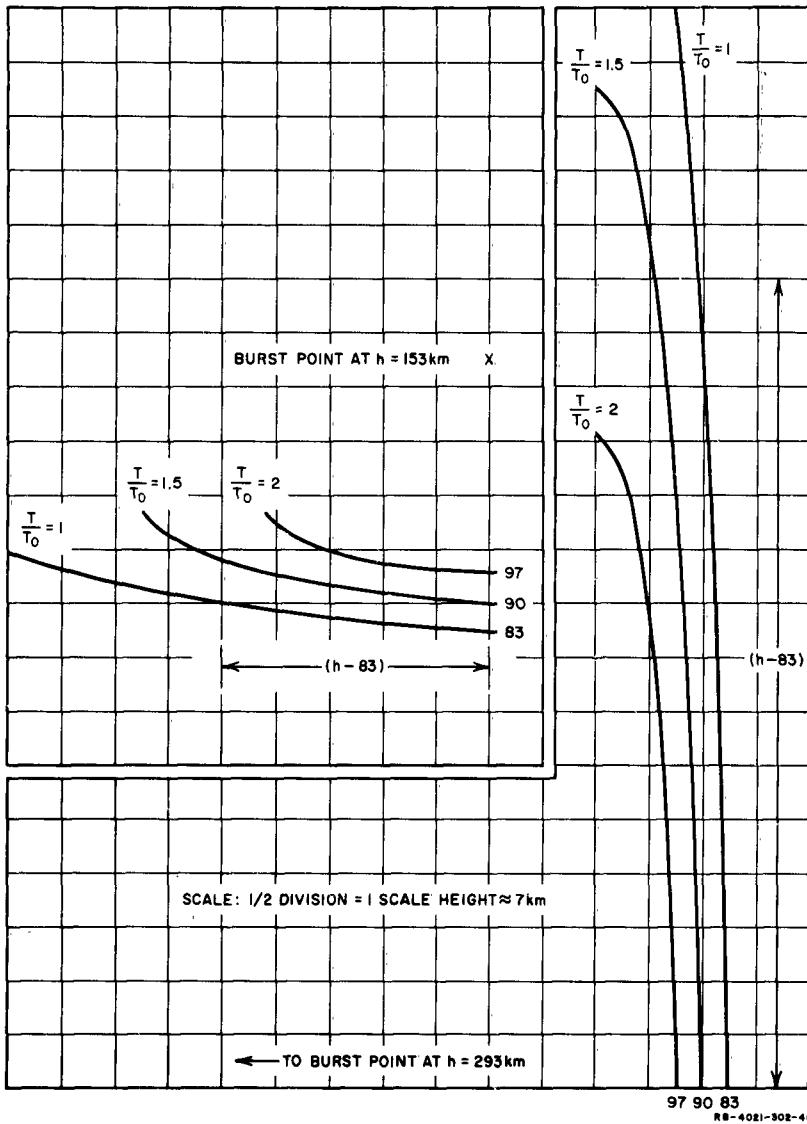
97 90 83

R8-4021-302-40

FIG. 12   ISOTHERMAL CONTOURS FOR ABOVE-THE-ATMOSPHERE DETONATIONS
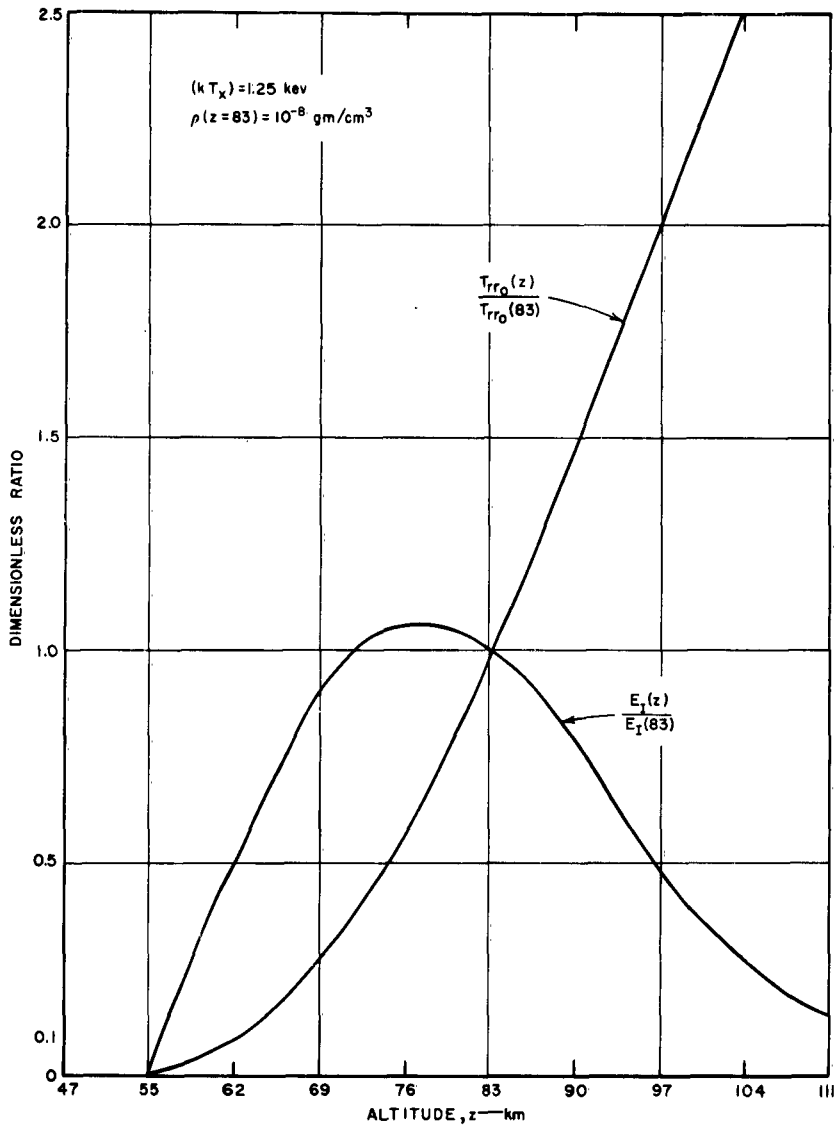AT TWO DETONATION HEIGHTS

FIG. 13 ENERGY AND TEMPERATURE DISTRIBUTION OF THE AIR DIRECTLY BELOW
AN ABOVE-THE-ATMOSPHERE DETONATION FOR AN INITIAL X-RAY
BLACK-BODY TEMPERATURE OF $(kT_x) = 1.25$ kev

32

change in the temperature dependence of the internal energy of air below 10^4 °K (see Eqs.(II-11) and (II-12)) the temperature distribution of Fig. 13 will decrease more sharply with decreasing altitude for the altitude range below the layer heated to 10^4 °K. However, the energy distribution curve will remain unchanged.

The area under the $E_I/E_I(83)$ curve in Fig. 13 is proportional to the incident x-ray energy flux from the device directly above ground zero, so that the fraction of this energy reradiated into the atmospheric passband will give the efficiency with which the x-rays are absorbed and then converted into radiation received on the ground.

To determine this efficiency it is first necessary to determine the temperature of the reradiating air. This is readily determined from Eqs.(II-17) and (II-18) and the temperature distribution plot of Fig. 13. For $(kT_x)=1.25$ kev, $z=83$ km, $\rho=10^{-8}$ gm/cm^3, there follows

$$T_{RR_o}^{\ \ 2}(83 \text{ km}) = \frac{9.2 \times 10^8 Y}{(h-83)^2} \quad (10^3 \text{ °K} < T < 10^4 \text{ °K}) \qquad (IV-13)$$

$$T_{RR_o}^{\ \ 3/2}(83 \text{ km}) = \frac{8.0 \times 10^6 Y}{(h-83)^2} \quad (T > 10^4 \text{ °K}) \qquad (IV-14)$$

where Y is in mt, h is in km, and T_{RR} is in °K. In Fig. 14, Y is plotted vs. h for $T_{RR_o} = 5 \times 10^3$, 10^4, and 2×10^4 °K.

In Fig. 15 is plotted the fraction of the total x-ray energy reradiated, E_R/E_I, for $T_{RR_o} = 2 \times 10^4$, 10^4, and 5×10^3 °K as a function of T. From Eqs.(III-19) through (III-22) an estimate for the time dependence of T can then be obtained for these three cases. From Eqs.(III-15) through (III-22) with $f = 2$ (corresponding to a thin radiating layer) it follows that it takes

$$\tau_1 = 0.09(\rho/10^{-8})^{-1.1} \text{ sec} \qquad (IV-15)$$

for the air to cool to 2×10^4 °K;

$$\tau_2 = 0.014(\rho/10^{-8})^{-1.1} \text{ sec} \qquad (IV-16)$$
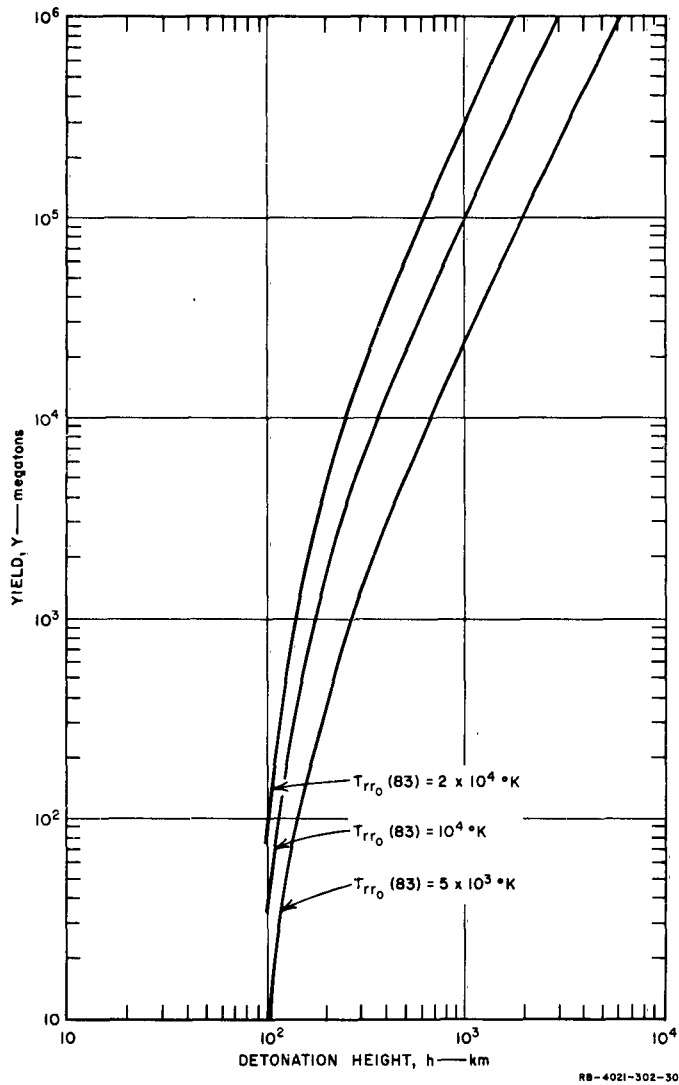
FIG. 14   YIELD REQUIRED AT A GIVEN HEIGHT TO GIVE AN INITIAL RERADIATION
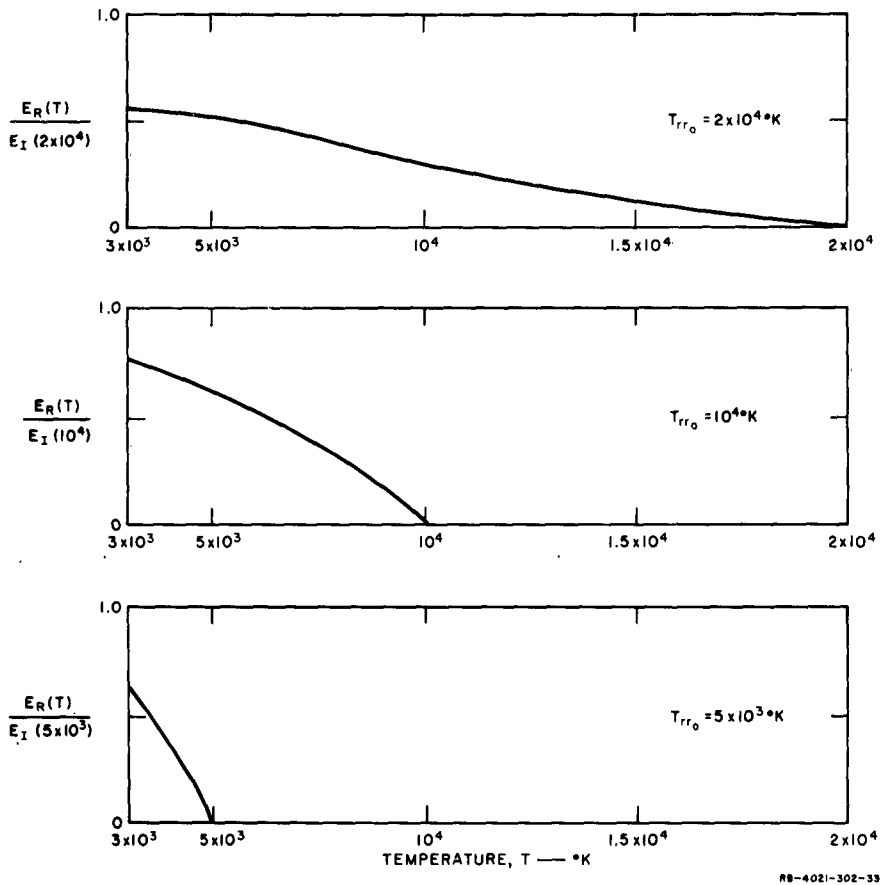TEMPERATURE AT 83 km ($\rho = 10^{-8}$ gm/cm^3) OF 5×10^3, 10^4, AND 2×10^4 °K

34

FIG. 15   FRACTIONAL ENERGY RADIATED FROM 2×10^4, 10^4, AND 5×10^3 °K
AIR MASSES AS A FUNCTION OF TEMPERATURE

for the air to cool from 2×10^4 to 1.5×10^4 $^\circ$K;

$$\tau_3 = 0.095(\rho/10^{-8})^{-0.6} \text{ sec} \qquad\qquad \text{(IV-17)}$$

for the air to cool from 1.5×10^4 to 10^4 $^\circ$K

$$\tau_4 = 0.125(\rho/10^{-8})^{-0.5}[(\frac{10^4}{T})^7 - 1] \text{ sec} \qquad\qquad \text{(IV-18)}$$

for the air to cool from 10^4 to T $^\circ$K; and

$$\tau_5 = 16(\rho/10^{-8})^{-0.5}[(\frac{5 \times 10^3}{T})^7 - 1] \text{ sec} \qquad\qquad \text{(IV-19)}$$

for the air to cool from 5×10^3 to T $^\circ$K.

To give an idea of the variation of reradiation efficiency with device yield Y, Table I gives a rough estimate of the fractional energy, ϵ, reradiated in the atmospheric passband in 0.1, 1.0, and 10 sec for $T_{RR_o} = 2.5 \times 10^3$, 5×10^3, 10^4, and 2×10^4 $^\circ$K.

Table I

FRACTION OF ABSORBED X-RAY ENERGY (ϵ) RERADIATED IN THE
ATMOSPHERIC PASSBAND IN 0.1, 1.0,
10 SEC

$T_{RR_o}(83)$	Time		
	0.1 sec	1.0 sec	10 sec
2×10^4 $^\circ$K	0.12	0.22	0.38
10^4 $^\circ$K	0.06	0.19	0.33
5×10^3 $^\circ$K	0	0.07	0.16
2.5×10^3 $^\circ$K	0	0	0.1

Table I was obtained by first determining from Fig. 13 the percentage energy and the average temperature of layers a scale-height thick (7 km) at the heights 69, 76, 83, 90, 97, and 104 km, and then from Eqs. (III-15) through (III-18), and Fig. 15 obtaining the fraction of the energy reradiated into the atmospheric passband within 0.1, 1.0, and 10 sec from each of these scale-height thick layers.

An estimate of the over-all efficiency within a given time is then obtained by multiplying the values given in Table I by 4/5 x 1/4 = 1/5 (4/5 of the device energy is assumed in x-rays and of that less than 1/4 is absorbed in the reradiating layers). As opposed to the UA detonation case in which the efficiency of transfer to the ground did not change with the yield for any yield greater than 5 mt, in the AA detonation both the efficiency and time dependence of the reradiation are functions of the temperature of the heated air as shown in Table I and thus are functions of the yield (as shown in Fig. 14).

To obtain a better estimate of the time dependence of the reradiated energy, Fig. 16 graphically presents the ϵ vs. time information of Table I. From a graphical differentiation of Fig. 16, Fig. 17 is obtained, giving the time dependence of $d\epsilon/dt$, which is directly proportional to the power reradiated to the ground. From this plot it is seen that for times greater than 1 sec, the power goes roughly as $t^{-1.3}$, in agreement with the fact that below 10^4 ^0K, air at the densities in question radiate energy as $t^{-9/7} = t^{-1.29}$ (see Eqs. (III-11), (III-15), (IV-3), and (IV-10).
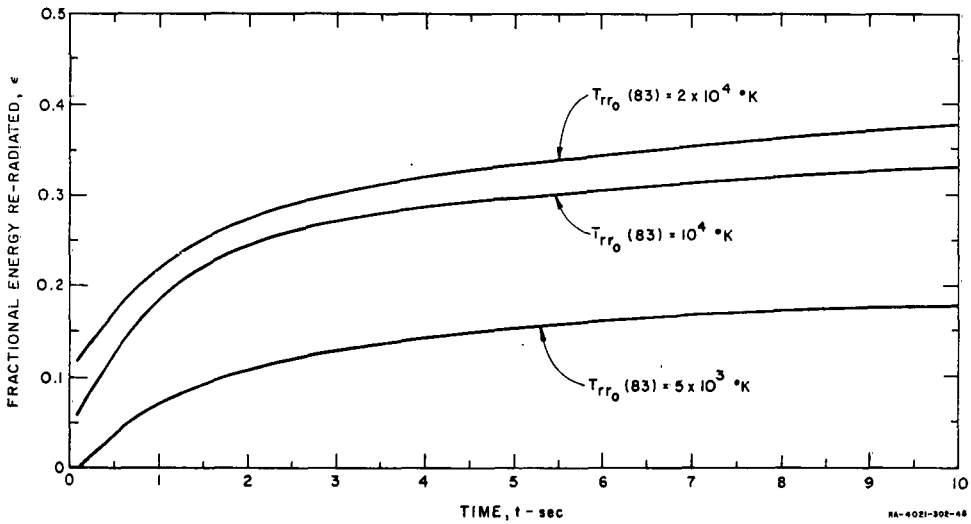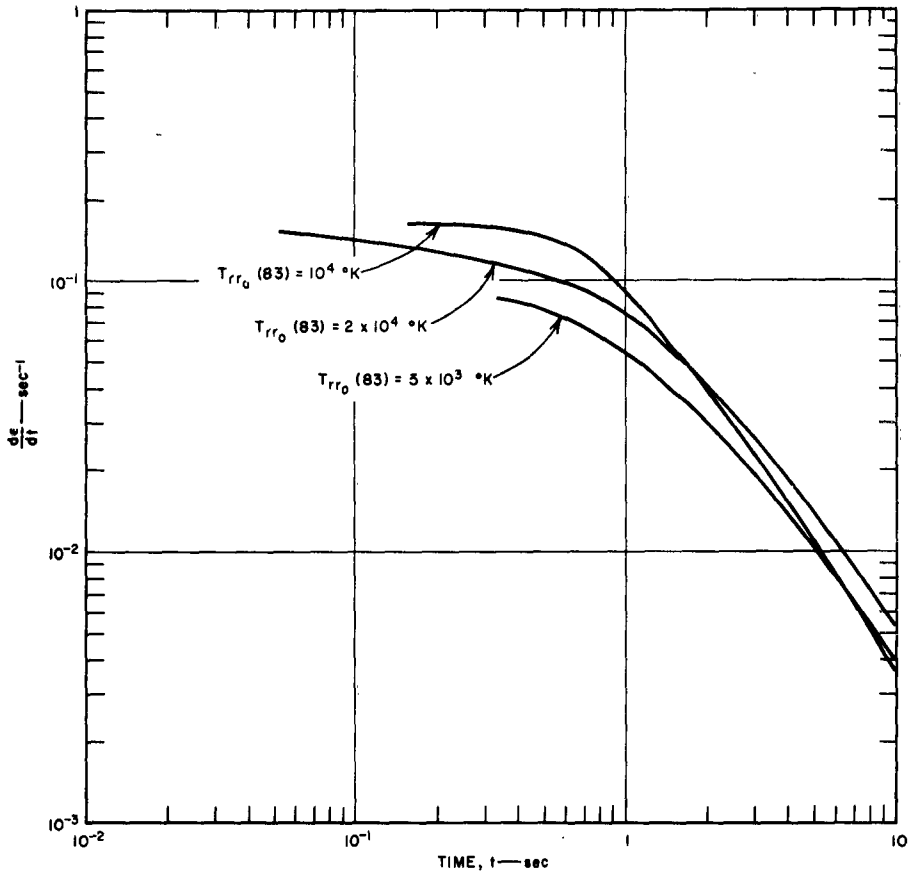
FIG. 16   FRACTIONAL ENERGY RADIATED FOR ABOVE-THE-ATMOSPHERE
DETONATIONS vs. TIME

FIG. 17   A QUANTITY PROPORTIONAL TO THE POWER RADIATED TO THE GROUND IN
ABOVE-THE-ATMOSPHERE DETONATIONS AS A FUNCTION OF TIME AFTER
DETONATION

39

V GEOMETRY AND TRANSMISSION FACTORS

The radiation received on the ground can now be determined from a consideration of the geometry factors involved and the transmission of the atmosphere.

For the UA detonation, the geometry factor is given simply by $(4\pi r^2)^{-1}$, where r is the distance from the detonation point to any other point in question. It will be convenient to consider the ground effects at those points on the ground n burst heights away from ground zero, for which case r^2 becomes

$$r_n^2 = (n^2+1)h^2, \tag{V-1}$$

where h is the burst height. If we let F_n represent the transmission factor corresponding to the path from the burst point (UA detonations only) to the ground point at nh, then the integrated energy flux, S_n^{UA}, received at the ground point n burst heights from ground zero on a surface normal to the ray to the detonation point is given by

$$S_n^{UA} = \frac{2 \times 10^3 \; F_n Y}{(n^2+1)h^2} \; cal/cm^2 \quad (h<80 \; km) \tag{V-2}$$

where Y is mt, h is in km, and an over-all efficiency of 25% for the conversion of the initial energy of the device into energy reradiated into the atmospheric passband has been assumed. In particular S_o^{UA} gives the effect at ground zero.

In AA bursts the geometry is slightly more complicated, since the reradiating surface approximates a flat circular cone rather than a sphere. To determine the ground zero effect it is considered (from the properties of a cone) that the reradiating layer has an average distance from ground zero given by

$$R_o^2 = \left(83^2 + \left[\frac{(h-83)}{2}\right]^2\right) \; km \tag{V-3}$$

since the reradiating air is centralized about a height of 83 km ($\rho = 10^{-8}$

gm/cm³), and the median radius of the conical pancake is approximately $\frac{1}{2}$(h-83) km. For a ground point (nh) km from ground zero, the reradiating volume can again (as for the UA detonation) be taken as concentrated at the center of the reradiating air, so that the distance from the reradiating air to the ground point is given by

$$R_n{}^2 = (83^2 + n^2 h^2) \text{km}^2 \quad (n > 1) \tag{V-4}$$

In Fig. 18 are plotted $h^2/R_o{}^2$, $R_o{}^2/R_1{}^2$, $R_o{}^2/R_2{}^2$, and $R_o{}^2/R_3{}^2$ as functions of h. The energy flux, $S_n{}^{AA}$, received at the ground point r_n normal to the ray to the center of the reradiating layer is thus given by

$$S_n{}^{AA} = \frac{1.6 \times 10^3 \, \epsilon(T_{RR_o})F'_n \, Y}{R_n{}^2} \quad \text{cal/cm}^2 \quad (h > 100 \text{ km}) \tag{V-5}$$

where Y is in mt, h is in km, and ϵ is given in Table I for various relevent times and representative initial reradiating temperatures, T_{RR_o}. (In Fig. 14, these initial temperatures, T_{RR_o}, are related to a required yield at a given burst height). $F'_n = F_n$ as defined in Eq. (V-1) for n>1; however $F' \neq F_o$, as F'_o is the transmission factor corresponding to the path from ground zero to the median radius of the reradiating layer, as given in Eq. (V-3).
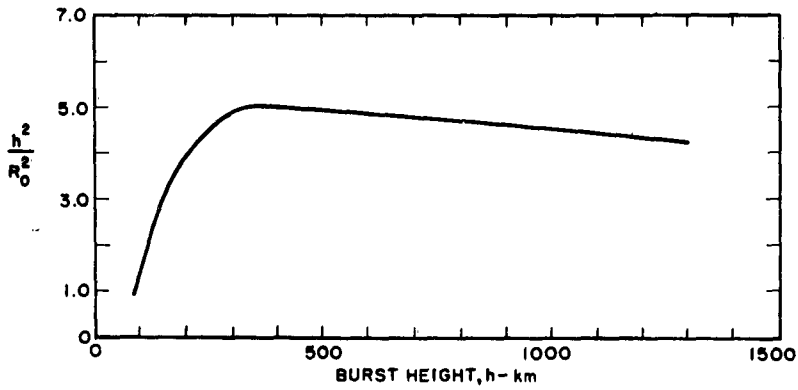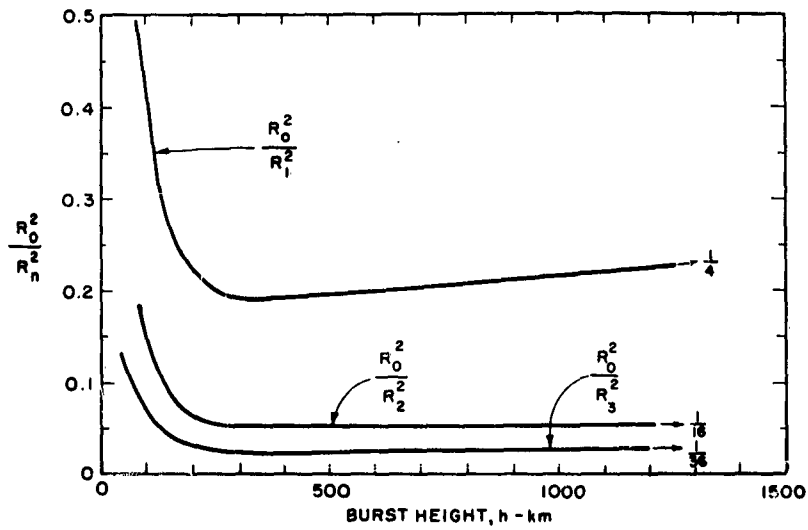
The ratio of the energy flux received at a ground point (nh) km away from ground zero to that energy flux received at ground zero is thus given by

$$\frac{S_n{}^{UA}}{S_o{}^{UA}} = \frac{F_n}{F_o} \times \frac{1}{(n^2+1)} \quad (h < 80 \text{ km}) \tag{V-6}$$

$$\frac{S_n{}^{AA}}{S_o{}^{AA}} = \frac{F_n}{F'_o} \times \frac{R_o{}^2}{R_n{}^2} \quad (h > 100 \text{ km}) \tag{V-7}$$

where $R_o{}^2/R_n{}^2$ and $1/(n^2+1)$ are plotted in Fig. 19 as a function of the distance on the ground from ground zero (in units of the burst height h for various representative burst heights).

FIG. 18 GEOMETRY FACTORS INVOLVED IN ABOVE-THE-ATMOSPHERE DETONATIONS
AS A FUNCTION OF THE DETONATION HEIGHT

43

The graph contains the following labels:

- Y-axis: $\dfrac{S_n/F_n}{S_0/F_0}$ with values 1.0, 0.8, 0.6, 0.4, 0.2, 0
- X-axis: DISTANCE FROM GROUND ZERO—burst heights, with values 0, 1, 2, 3, 4
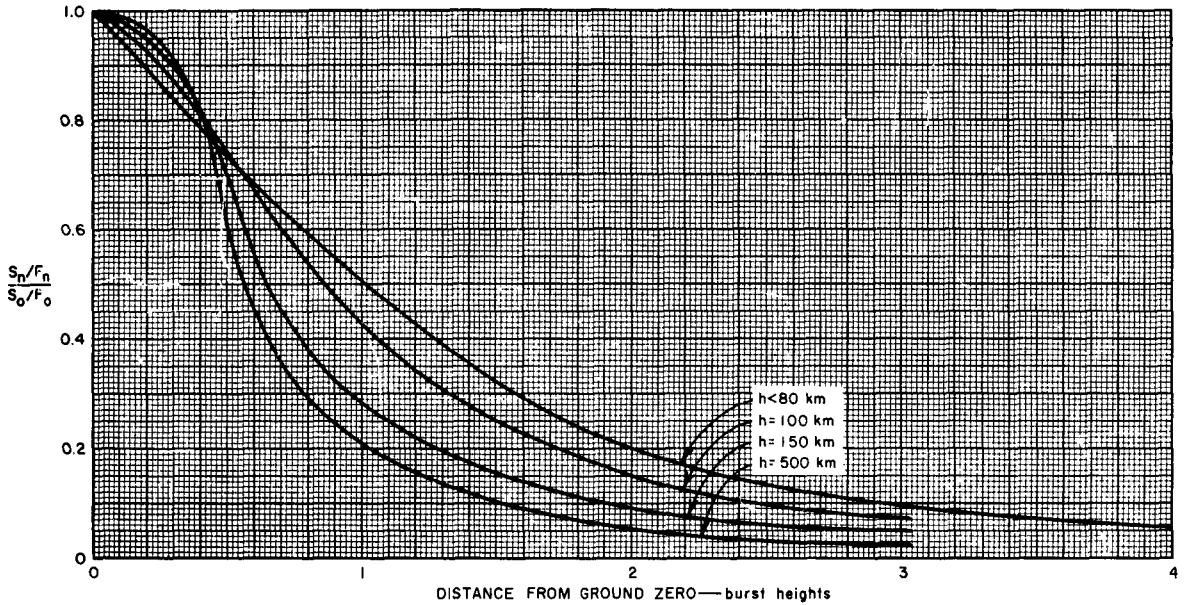- Legend: h<80 km, h=100 km, h=150 km, h=500 km
- RB-4021-302-41

FIG. 19   THE RADIAL DISTRIBUTION OF THE ENERGY FLUX RECEIVED ON THE GROUND AS A FUNCTION OF THE DISTANCE FROM GROUND ZERO

VI   GROUND EFFECTS CURVES

In Fig. 20 is plotted the yield as required by Eqs. (V-2) and (V-5) at any given burst height h greater than 50 km to give 5 cal/cm^2, 10 cal/cm^2, and 100 cal/cm^2 at ground zero. The atmospheric transmission factors are neglected in these plots, and a reradiation efficiency for absorbed x-ray energy, ϵ, of 1/5 is assumed (see Table I) for AA detonations. This value of ϵ corresponds to an overall efficiency of 1/5 x 1/5 = 1/25.

Superimposed upon these curves are the yield vs. detonation height plots for a given initial reradiation temperature, T_{RR_o} (83), as presented in Fig. 14. From an inspection of where the Y vs. h curve for a required S_o falls with respect to the Y vs. h curves for a given T_{RR_o}, a rough estimate of the initial reradiation temperature of the heated air can be made and then, by reference to Table I, a better estimate of the actual reradiation efficiency, ϵ, can be used to correct the value of S_o stated on the curve in question. All ground zero effect curves lying to the right of the $T_{RR_o} = 5 \times 10^3$ °K curve must be considered as very questionable because of the extremely slow radiation times of the reradiating air when heated to initial temperatures lower than 5×10^3 °K.

The following items summarize the chief features of Fig. 20 which must be kept in mind in deducing ground effects.

  a. For all altitudes below 80 km, the S_o curves are used
      at face value (without multiplying by a factor in the
      bracket label appropriate to the 2×10^4 °K curve).

  b. Using only the intersections of yield and temperature
      curves assures greater certainty of (1) the power pulse
      time behavior, (2) the total energy in the pulse.

  c. It is to be noted that the value on each S_o curve in
      Fig. 20 is directly proportional to yield. The reason
      is that a constant ϵ (namely 1/5) was assumed for the
      AA portions above 80 km. The constant $\epsilon = 0.25$ is
      used for the UA portions of the S_o curves.

  d. Points in the region to the right of the 5000°K tempera-
      ture curve are not considered significant and should not
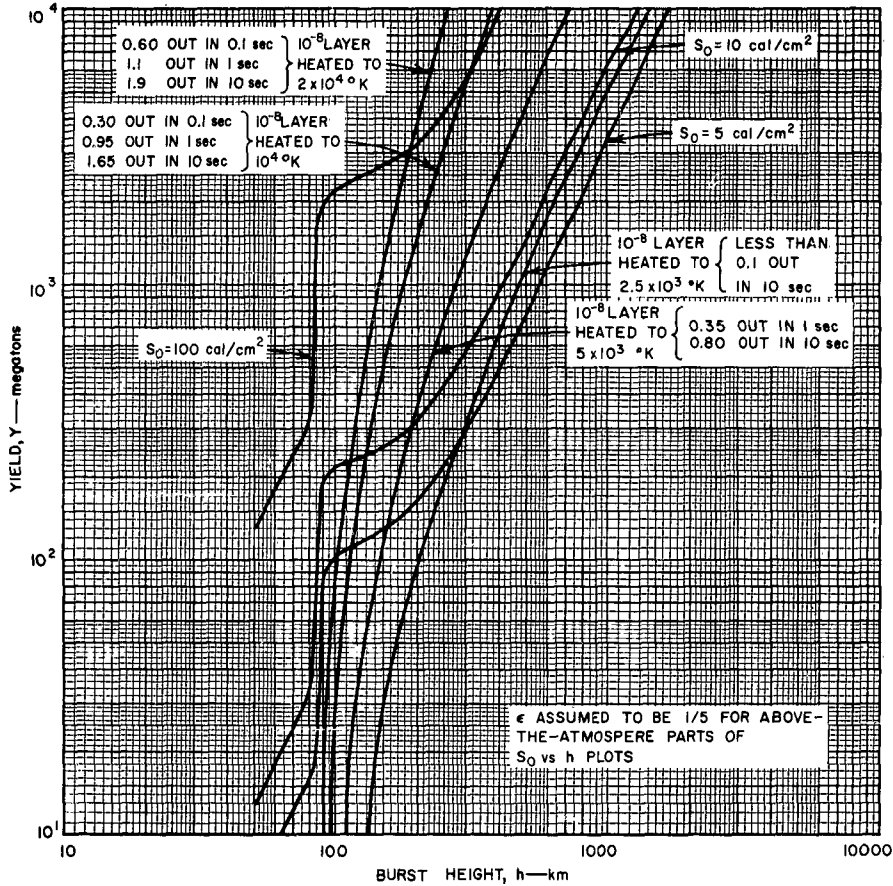   be used to calculate ground effects.

FIG. 20   THE YIELD REQUIRED AT A GIVEN HEIGHT FOR ENERGY FLUXES OF 100, 10, AND 5 cal/cm² AT GROUND ZERO (Neglecting Atmospheric Attenuation)

e. Points to the left of the 2×10^4 $^\circ$K curve may be considered
    to exhibit identical time behavior to those on that curve.

f. The values of cal/cm^2 on the S_o curves are for surfaces
    oriented perpendicular to the ray from the centroid of
    the reradiating layer.

g. The curves of Fig. 20 cannot be extrapolated to altitudes
    below 50 km.

h. The bracketed labels for the temperature curves are
    correction factors to multiply the values on the S_o
    curves (or values interpolated between them) for times
    of 0.1, 1.0, and 10 sec.

i. It is unlikely that the radiation will persist to 10 sec
    because of loss of energy by hydrodynamic expansion of
    heated air layer.

In Fig. 21 the circle radius on the ground within which 5 cal/cm^2
is received within 10 sec (neglecting atmospheric transmission factors)
is plotted against detonation height for yields of 100, 1000, and 10,000
mt. These curves are obtained from Figs. 19 and 20 by the following
procedure:

a. Locate one of the three intersections of a temperature
    curve ($>5 \times 10^3$ $^\circ$K only) in Fig. 20 with the yield-horizontal
    under consideration. For 100 mt, these intersections are
    at 100, 110, and 145 km for the 2×10^4 $^\circ$K, 10^4 $^\circ$K, and
    5×10^3 $^\circ$K curves, respectively.

b. Taking first the intersection at h=145 km, Y=100 mt,
    T=5×10^3 $^\circ$K one sees that 128 mt is required to give 5
    cal/cm^2 at ground zero. However, the bracket label
    on the 5×10^3 $^\circ$K curve shows that only 0.8x5=4 cal/cm^2
    is received in 10 sec. It is thus clear that h=145 km
    is too high an altitude to deliver 5 cal/cm^2 at ground
    zero, and is not a point on the 5 cal/cm^2 circle.

c. Proceeding to the Y=100 mt, h=110 km, T=10^4 $^\circ$K inter-
    section and noting on the curve for S_o=5 cal/cm^2 (at
    110 km) that 110 mt is required, then 100 mt gives
    100/110 x 1.65 x 5 = 7.5 cal/cm^2 at ground zero in
    10 sec.

d. The radial distribution cueves of Fig. 19 are now used
    to find the number of burst heights from ground zero at
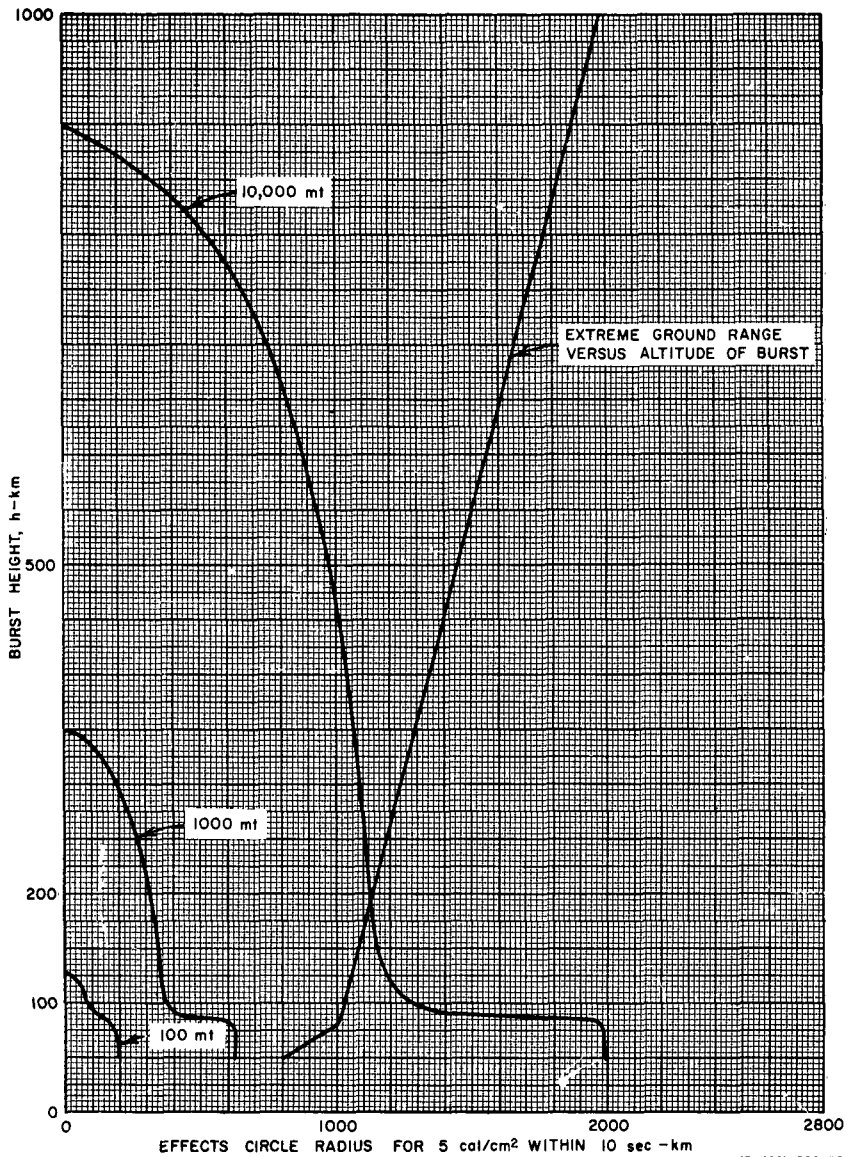   which a ground zero value of 7.5 has been reduced to
    5 cal/cm^2.

FIG. 21 UPPER LIMIT TO RADIUS OF CIRCLE ON GROUND ALONG WHOSE PERIMETER
IS RECEIVED 5 cal/cm^2 WITHIN 10 sec AS A FUNCTION OF DETONATION
HEIGHT FOR YIELDS OF 100, 1000, AND 10,000 mt

48

e. Since 5/7.5=0.67, one follows the ordinate 0.67 in
       Fig. 19 to the curve closest to the altitude in question.
       Using the 100-km curve as a reasonable approximation to
       110 km, the perimeter radius is 0.6 h or 0.6x110=66 km.

We have just obtained one point on the 5 cal/cm^2 (in 10 sec) circle
radius vs. burst altitude profile for a 100-mt detonation. Points for
5 cal/cm^2 arriving within 1 sec or 0.1 sec can be similarly obtained.

A noteworthy point about the circle radius-altitude profiles of
Fig. 21 is their assumption of a flat earth. Therefore, plotted with
the profiles of Fig. 21 is the extreme ground range as a function of
altitude. Since the radiating layer seen from the earth is never higher
than about 80 km, (corresponding to an extreme ground range of 1000 km)
the profiles at ground effects circle radii > 1000 + (h-80) km are not
significant, where (h-80) is the approximate radius of the radiating
layer.

49

VII CONCLUSIONS

The existence of a fireball ceiling in the altitude region around 80 km is perhaps the primary conclusion of this study. That is, regardless of the burst altitude the incandescent region capable of radiating within the atmospheric transparency window cannot be above ~80 km for initial detonation temperatures around 10^7 °K.

Fireball shape undergoes a sharp change as the burst height increases above about 80 km. Below 80 km the fireball is approximately spherical. Above 80 km burst height the fireball assumes the approximate shape of a flat circular disk centered about the 80-km level and parallel to the earth's surface. The radius of the disk is roughly equal to the burst height in km minus 80.

An 80-km upper limit for the fireball (or fire disk) altitude is an important restriction on the area of the earth's surface which can receive radiant energy. This restriction comes about from the fact that the extreme limit of the ground range from a point at 80-km altitude is about 1000 km. Since atmospheric absorption has been negelected, the radius of the largest perimeter of irradiated earth from a single detonation is in fact always less than 1000 km.

There is a marked change in the efficiency for energy transfer from bursts that occur around 80-km altitude. For bursts below 80-km altitude (and above 50 km) intense thermal pulses less than 1-sec long occur at ground level for all yields above a few megatons. Within the 10 or 20 km above 80 km, the efficiency for conversion of energy to that which can reach the earth's surface suddenly drops from ~25% to ~5%. A further increase in altitude diminishes this efficiency even more so that eventually the only thermal radiation received at the ground is the flash fluorescence (a few microseconds in length) which has an efficiency ~1.5%. (See Appendix.)

Aside from a purposeful attempt to establish upper limits to ground effects throughout the study, the major uncertainty in the study is the assumption of thermal equilibrium within the incandescent layer, especially for detonations above 80 km. It is the authors' opinion that

this uncertainty will only be resolved by an experimental program to determine how fast x-ray flash-heated air reaches thermal equilibrium.

The next step which logically follows the present study is one which assesses the effects of atmospheric attenuation on thermal ground effects. Such a step has been taken and has resulted in another report to be published simultaneously with the present one.[14]

APPENDIX A

FLUORESCENCE AND N_2^+ RADIATION

Photons in the x-ray energy range, when absorbed in air, lose their energy by photoejection of fast primary electrons from the air atoms and molecules. These electrons then lose their energy in ionizing, dissociating, and exciting air molecules and atoms. It is well known that it takes about 34 ev to form an ion pair in air. Of the ions so formed, 62.5% are N_2^+ with N^+, O_2^+, and O^+ making up the remaining 27.5%.[11] In the formation of these ions, some of the molecules are left in excited states and thus radiate energy in returning to their ground states. The fluorescent energy efficiency in air of the first positive N_2^+ band at 3914A has recently been measured[12] as 3.3×10^{-3}. Also calculated has been an over-all fluorescent efficiency of 1.5×10^{-2} in the wavelength range from 3000 to 10,000A.[12] This radiation will be emitted in the lifetimes of the atomic states in question, which in most cases is less than one microsecond. Thus about $1\frac{1}{2}\%$ of the x-ray energy from a nuclear detonation is emitted as fast fluorescence, the so-called "Teller light."

When detonations above the atmosphere do not deposit sufficient energy in the lower lying air to heat it to a significant radiating temperature (greater than $5 \times 10^3 \ {}^\circ K$), fluorescence will be a major effect. From Fig. 14, it is seen that this is true for all AA detonations with yields less than 100 mt. For any AA detonations that could produce a ground zero effect of greater than 5 cal/cm^2, however, the black-body reradiation of the heated air is a greater effect than the fluorescence, and so the fluorescence can then be neglected. This assumes that the time behavior difference between fluorescence and thermal emission is not significant.

Because N_2^+ is the dominant radiating species in heated air at thermodynamic equilibrium in the temperature range from 5×10^3 to $10^4 \ {}^\circ K$, the possibility was considered that the equilibrium radiation rate could be enhanced by those N_2^+ ions formed in much greater than equilibrium concentration by the ionizing primary electrons. The lifetime, however, for the three body recombination reaction

$$N_2^+ + e^- + X \rightarrow N_2 + X \qquad\qquad\qquad (A\text{-}1)$$

is sufficiently short[13] (10^{-4} seconds at $\rho=10^{-8}$ gm/cm^3, T=2x10^4 $^\circ$K, electron density=air density) that for significant radiation times the N_2^+ ions can be considered in equilibrium concentration.

Actually the reaction

$$N_2^+ + e^- \rightarrow N + N \qquad\qquad\qquad (A\text{-}2)$$

is the more probable mode of recombination. With this mode, the recombination time at the N_2^+ and electron concentration level of 10^{-7} times the original air density is about 10^{-7} sec. The 10^{-7} relative concentration level is ten times the equilibrium concentration at $\rho=10^{-8}$ g/cm^3, and T=12x10^3 $^\circ$K. The above recombination time is calculated from the equation

$$\frac{dN}{dt} = -\alpha[N_2^+][e^-]$$

where dN/dt is the decay rate of either species, α is the recombination coefficient in cm^3/sec (taken to be $\sim 10^{-7}$), $[N_2^+]$ is the concentration in particles/cm^3 of N_2^+ ions and $[e^-]$ the similar quantity for electrons.

It can be concluded that recombination rates are sufficiently high to assure N_2^+ populations roughly equal to the values for air in thermodynamic equilibrium over times after the first few microseconds after detonation. A negligible fraction of the total thermal radiant emission occurs within times of this order.

REFERENCES

1. Glasstone, S., The Effects of Nuclear Weapons, U.S. Government Printing Office (1962)

2. Kerr, N. A., Determination of Certain Spectral Distributions of Soft X-Rays by Theoretical Analysis of Absorption Experiments, J. Appl. Phys. 32, 2465 (Nov., 1961)

3. Gilmore, F. R., Equilibrium Composition and Thermodynamic Properties of Air to 24,000°K, Rand Corporation, RM-1543 (August 1955)

4. Chandrasekhar, S., An Introduction to the Study of Stellar Structure, Dover, New York (1957)

5. Meyerott, R. E. and J. Sokoloff, Absorption Coefficients of Air, Lockheed Aircraft Corp. Missiles and Space Division, LMSD-288052 (Sept. 1959)

6. Armstrong, B. H., D. H. Holland, and R. E. Meyerott, Absorption Coefficients of Air from 22,000° to 220,000°, AFSWC-TR-58-36 (August 1958)

7. Kivel, B. and K. Bailey, Tables of Radiation from High Temperature Air, AVCO Research Report, RR 21 (1957)

8. Handbook of Geophysics, MacMillan, New York (1960)

9. Weissler, G. L. and P. Lee, J. Opt. Soc. Am. 42, 200 (1952)

10. Pivovonsky, M. and M. R. Nagel, Tables of Black Body Radiation Functions, MacMillan, New York, (1961)

11. Meyerott, R. E., R. K. M. Landshoff, and J. Magee, Physics of the Ionization Processes in Air, Lockheed Aircraft Corp. Missiles and Space Division, LMSD-48361 (Dec. 1958)

12. Hartman, P. L. and H. Hoerlin, Measurements of the Fluorescence Efficiency of Air under Electron Bombardment, Bull. of the Am. Phys. Soc., Ser.II, Vol.7, No.1, p.69 (Jan. 1962)

13. Massey, H. S. W. and E. H. S. Burhop, Electronic and Ionic Impact Phenomena, Oxford (1952)

14. Passell, T. O., Transmission by the Earth's Atmosphere of Thermal Radiation from Nuclear Detonations above 50-km Altitude, to be published as part of the work under Contract OCD-OS-62-135(III), 1963

GLOSSARY OF TERMS

(in order of occurrence)

mt	energy equivalent to a detonation of 1 megaton of TNT, namely 4×10^{22} ergs
km	kilometers
^{0}K	degrees Kelvin
AA	above-the-atmosphere (above 80 km)
UA	upper-atmosphere (50-80 km)
μ_{x-ray}	absorption coefficient for x-rays in $cm^2/gram$
E	energy of x-rays (usually in kiloelectron volts)
ρ	density of air (gm/cm^3)
Z	altitude (kilometers)
I	x-ray energy flux $(ergs/cm^2)$
I(X)	x-ray energy transmitted a thickness X into an absorber
X	absorber thickness (usually in units of gms/cm^2)
F(E)	x-ray energy spectrum
T	temperature
T_x	temperature representative of the initial x-ray flash from a detonation
k	Boltzmann constant 8.62×10^{-8} kev/^{0}K
u	dimensionless quantity equal to E/kT_x
ARDC atmosphere	Standard atmosphere chosen by the Air Research and Development Command as the basis for all ARDC designs
$\mu(kT_x)X$	number of attenuation lengths for monoenergetic x-rays of energy kT_x
$P(\vec{b}, \vec{r})$	mass surface density (gm/cm^2) along a path from a given burst point b $(0,0,h)$ to a point of interest r (r, θ, Z)

$L_{1/e}$ — path length over which x-ray energy is reduced to 1/e of its initial value

E_I — internal energy density of heated air (ergs/cm³)

T_{RR_o} — temperature at time zero of the volume of air wherein the energy of the initial x-ray flash is deposited

Y — yield of a nuclear detonation (megatons TNT)

$A(T_x, P(Z))$ — differential x-ray energy absorbed per unit mass density for a Planck photon distribution described by the temperature T_x, at a depth $P(Z)$

$\dfrac{(kT_x)^3}{A(T_x, P(Z))}$ — quantity proportional to the detonation yield required to heat air at altitude Z to some fixed temperature T_{RR_o} for a given burst height, h

N_υ — energy flux emitted by a body per unit solid angle, per unit projected area of the body's surface, per unit photon frequency interval (ergs-cm⁻²-sec⁻¹-(unit frequency in sec⁻¹)⁻¹-sterad⁻¹

μ_υ — absorption coefficient of radiation of frequency υ (cm⁻¹)

μ'_υ — absorption coefficient of radiation of frequency υ corrected for induced emission

s — distance along a path within heated air layer or sphere (cm)

h — Planck's constant 6.62×10^{-27} erg-sec (usually appears as $h\upsilon$)

υ — frequency of electromagnetic radiations (sec⁻¹)

B_υ — black-body energy spectrum $= 2\dfrac{h\upsilon^3}{c^2}(\exp(h\upsilon/kT)-1)^{-1}$

$I(s)$ — total radiant energy crossing the surface element dA of the radiating surface at s, per unit area per unit time

$\bar{\mu}$ — mean absorption coefficient averaged over the Planck black-body distribution

f — factor by which $\bar{\mu}\sigma T^4$ is multiplied to give the volume energy emission rate for the two radiating shapes considered, a sphere ($f=3$) and a flat disc ($f=2$)

E_R	energy radiated into the atmospheric passband
t'	time for fireball to reach roughly uniform temperature of 10^4 ^{0}K = $t_1 + t_2 + t_3$
t_1	time for the UA fireball to cool to 2.5×10^4 ^{0}K, however hot initially
t_2	time for the UA fireball to cool from 2.5×10^4 ^{0}K to 1.5×10^4 ^{0}K
t_3	time for the UA fireball to cool from 1.5×10^4 ^{0}K to 10^4 ^{0}K
t_4	time for the UA fireball to cool from 10^4 ^{0}K to 3×10^3 ^{0}K
$\ell_{1/e}$	mean free path for cold oxygen absorption
x	the exponent in the equation t^{-x} giving the time dependence of the power pulse prior to the time the fireball cools to 10^4 ^{0}K
Z_o	altitude in kilometers directly above ground zero
θ	angle between vertical and the line from detonation point to a point in the reradiating layer
τ_1	time for reradiating pancake to cool to 2×10^4 ^{0}K, however hot initially (AA detonations)
τ_2	time for reradiating pancake to cool from 2×10^4 ^{0}K to 1.5×10^4 ^{0}K (AA detonations)
τ_3	time for reradiating pancake to cool from 1.5×10^4 ^{0}K to 10^4 ^{0}K (AA detonations)
τ_4	time for reradiating pancake to cool from 10^4 ^{0}K to T^0K (AA detonations)
τ_5	time for reradiating pancake to cool from 5×10^3 ^{0}K to T^0K
$\mathcal{E}$	E_R/E_I = fractional part of the x-ray energy which is reradiated in the atmospheric passband
r_n	path from center of radiating fireball to a point on the ground n burst heights from ground zero
n	number of burst heights

S_n^{UA} integrated energy flux received at the ground point n burst heights from ground zero on a surface normal to the ray from the detonation point in the upper atmosphere (50-80 km)

S_n^{AA} integrated energy flux received at the ground point n burst heights from ground zero on a surface normal to the ray from the center of the radiating layer for AA detonations (>80 km)

S_o integrated energy flux to a horizontal surface at ground zero

R_o effective path length to ground zero from the reradiating layer

R_n effective path length from reradiating layer to a ground point n burst heights from ground zero

F_n atmospheric transmission factor for a path from reradiating layer to points n burst heights from ground zero

F_o atmospheric transmission factor for path to ground zero from reradiating fireball (UA only)

F_o' atmospheric transmission factor for path to ground zero from reradiating layer (AA only)

ASTIA NO.

STANFORD RESEARCH INSTITUTE, Menlo Park, California

RADIATIVE ENERGY TRANSFER FROM NUCLEAR DETONATIONS ABOVE 50-km ALTITUDE, by R. I. Miller and T. O. Passell. April 30, 1963, 78 p. incl. illus., tables.

(Project 4021-302 Task III) [OCD-OS-62-135 (III)] Unclassified Report

The thermal energy flux expected at optimally oriented surfaces at the earth's surface from nuclear bursts detonated above 50 kilometers altitude has been computed from basic physical principles. The chief principles involved are a) absorption by the earth's atmosphere of a black-body X-ray spectrum from a point source near 10⁷ °K; b) heating of air to some temperature depending upon its known internal energy-temperature function; c) radiative cooling of the heated air assuming thermal equilibrium;

d) disposition of the radiant emission into three energy bands; cold oxygen absorption band, ozone absorption band, and the atmospheric passband.

d) disposition of the radiant emission into three energy bands; cold oxygen absorption band, ozone absorption band, and the atmospheric passband.

d) disposition of the radiant emission into three energy bands; cold oxygen absorption band, ozone absorption band, and the atmospheric passband.

d) disposition of the radiant emission into three energy bands; cold oxygen absorption band, ozone absorption band, and the atmospheric passband.

STANFORD RESEARCH INSTITUTE

MENLO PARK CALIFORNIA

Regional Offices and Laboratories

Southern California Laboratories
820 Mission Street
South Pasadena, California

Washington Office
808 17th Street, N.W.
Washington 6, D.C.

New York Office
270 Park Avenue, Room 1770
New York 17, New York

Detroit Office
1025 East Maple Road
Birmingham, Michigan

European Office
Pelikanstrasse 37
Zurich 1, Switzerland

Japan Office
911 Iino Building
22, 2-chome, Uchisaiwai-cho, Chiyoda-ku
Tokyo, Japan

Representatives

Honolulu, Hawaii
1125 Ala Moana Blvd.
Honolulu, Hawaii

London, England
19, Upper Brook Street
London, W. 1, England

Milan, Italy
Via Macedonio Melloni, 49
Milano, Italy

Toronto, Ontario, Canada
Room 710, 67 Yonge St.
Toronto, Ontario, Canada